Competition for a limited pool of cohesin between centromeres and the rDNA triggers chromosomal instability that shortens replicative lifespan

Ryan D. Fine[1], Nazif Maqani[1], Mingguang Li[1,2], Elizabeth Franck[1], and Jeffrey S. Smith[1,*]

[1]Department of Biochemistry and Molecular Genetics, University of Virginia School of Medicine, Charlottesville, VA 22908. [2]Department of Laboratory Medicine, Jilin Medical University, Jilin, 132013, China

[*]Corresponding Author

Department of Biochemistry and Molecular Genetics

University of Virginia School of Medicine

Pinn Hall, Box 800733

Charlottesville, VA 22908

Phone: 434-243-5864

Fax: 434-924-5069

Email: jss5y@virginia.edu

Keywords: Sir2, Hst1, Mcd1, cohesin, Net1, RENT, Lrs4, monopolin, replicative lifespan, chromosome instability, rDNA, aging

Abstract

Sir2 is a highly conserved NAD^+-dependent histone deacetylase that functions in heterochromatin formation and promotes replicative lifespan (RLS) in the budding yeast, *Saccharomyces cerevisiae*. Within the yeast rDNA locus, Sir2 is required for efficient cohesin recruitment and maintaining stability of the tandem array. In addition to the rDNA, ChIP-seq of an epitope-tagged cohesin subunit (Mcd1-13xMyc) in a *sir2*Δ mutant revealed subtle reductions of cohesin binding at all 16 centromeres. Coupled with the previously reported chromosome instability in *sir2*Δ cells and depletion of Sir2 in aged cells, we hypothesized that mitotic chromosome instability (CIN) due to Sir2 depletion could be a driver of replicative aging. In addition to Sir2, we discovered that other subunits of the Sir2-containing SIR and RENT complexes were depleted in aged cells, as were subunits of the cohesin and monopolin/cohibin complexes, implying the possibility of CIN. ChIP assays of the residual Mcd1-13xMyc in aged cells showed strong depletion from the rDNA and possible redistribution to centromeres, most likely in an attempt to maintain chromosome stability. Despite the shift in cohesin distribution, sister chromatid cohesion was partially attenuated in old cells and the frequency of chromosome loss was increased. This age-induced CIN was exacerbated in strains lacking Sir2 and its paralog, Hst1, but suppressed in strains that stabilize the rDNA array due to the deletion of *FOB1* or through caloric restriction (CR). Furthermore, ectopic expression of *MCD1* from a doxycycline-inducible promoter was sufficient to suppress to rDNA instability in aged cells and to extend RLS. Taken together we conclude that age-induced depletion of cohesin and multiple other nucleolar chromatin factors destabilize the rDNA locus, which then results in general CIN and aneuploidy that shortens RLS.

Author summary

The aging process is generally characterized by the breakdown of multiple cellular processes, including the maintenance of genome integrity. Alterations from the normal chromosome number is known as aneuploidy, and commonly occurs in oocytes (eggs) of older mothers. The risk of aneuploidy increases with age and can cause diseases such as Down's syndrome (chromosome 21 trisomy). It is therefore important to understand how aging causes the chromosome instability (CIN) that leads to aneuploidy. In this study we have investigated whether CIN is associated with aging of mitotic cells using the budding yeast, *Saccharomyces cerevisiae*, as a model system. We show that chromosomes are indeed lost during aging of these cells due to the depletion of several key proteins that function in organizing and maintaining chromosome architecture, including the cohesin complex. Restoring cohesin levels was sufficient to delay aging, and adding extra cohesin even extended normal lifespan. Lastly, caloric restriction (CR), a dietary modification known to extend lifespan of yeast and other model organisms, strongly prevented chromosome instability, suggesting a possible new mechanism for how CR delays age-associated conditions at the cellular level.

57 **Introduction**

58 Budding yeast replicative lifespan (RLS) was originally described decades ago as the number of
59 times a mother cell divides before losing viability [1], and has been an effective model system
60 for the identification and/or characterization of several conserved aging-related genes and
61 pathways, including *SIR2*, AMPK (Snf1), and TOR signaling [2]. *SIR2* is probably the most
62 famous yeast gene associated with replicative aging and encodes the founding family member of
63 the NAD^+-dependent histone/protein deacetylases, commonly known as sirtuins (reviewed in
64 [3]). The NAD^+ dependence of sirtuins provides a direct link between metabolism and cellular
65 processes regulated by these enzymes. In fact, recent evidence points to depletion of cellular
66 NAD^+ pools as a potential mechanism for aging-associated disease, which could be mediated by
67 impairment of sirtuins or other NAD^+ consuming enzymes [4]. Therefore, understanding how
68 sirtuins are impacted by aging and determining how they contribute to the regulation of age-
69 altered cellular processes is of intense interest in the aging field.

70 Eukaryotic genomes generally encode for several different sirtuin homologs. The
71 *Saccharomyces cerevisiae* genome, for example, encodes *SIR2* and four additional Homologs of
72 Sir Two (*HST1-HST4*) [5]. Sir2 was originally shown to establish and maintain silencing of the
73 silent mating loci, *HML* and *HMR*, along with its fellow Silent Information Regulator (SIR)
74 proteins, Sir1, Sir3, and Sir4 [6]. Additionally, Sir2, Sir3, and Sir4 form the so-called SIR
75 complex that is recruited to and then spreads across the *HM* loci and telomeres to form
76 hypoacetylated heterochromatin-like domains (reviewed in [7]). Sir2 protein levels are
77 significantly reduced in replicatively old yeast cells [8], presenting a possible mechanism for the
78 decline of Sir2-dependent processes during aging, including gene silencing. Indeed, depletion of
79 Sir2 in old cells causes hyperacetylated H4K16 and silencing defects at subtelomeric loci [8].

80 Haploid cells lacking Sir2 derepress *HML* and *HMR*, resulting in co-expression of mating type
81 regulatory genes that together induce a diploid-like gene expression pattern that produces a non-
82 mating "pseudodiploid" phenotype [6]. Old haploid mother cells are sterile, presumably due to
83 the pseudodiploid effect [9], but more recent experiments point toward a silencing-independent
84 mechanism caused by aggregation of the Whi3 protein and loss of pheromone sensitivity [10].
85 Alternative models for Sir2 control of RLS have focused on the rDNA tandem array. Sir2
86 functions in the silencing of RNA polymerase II-dependent transcription at the rDNA locus on
87 chromosome XII via a nucleolar complex called RENT [11, 12], which consists of Sir2, Net1,
88 and Cdc14 [13, 14]. RENT-dependent H3 and H4 deacetylation represses transcription of
89 endogenous non-coding RNAs from the intergenic spacer (IGS) regions [15]. Derepression of
90 the bidirectional promoter (E-pro) within IGS1 of *sir2*Δ cells displaces cohesin from the rDNA,
91 thus destabilizing the array by making it more susceptible to unequal sister chromatid exchange
92 [16]. A predominant model for *SIR2* control of replicative aging postulates that
93 extrachromosomal rDNA circles (ERCs) derived from these unequal recombination events
94 specifically accumulate to high levels in mother cells, consequently causing cell death through an
95 unknown mechanism [17]. Such an ERC-centric model is supported by the extended RLS
96 extension of *fob1*Δ strains [18]. Fob1 binds to the rDNA in IGS1 to block DNA replication forks
97 from colliding with RNA polymerase I transcribing in the opposite direction [19]. The blocked
98 replication forks can collapse and result in double-stranded DNA breaks that trigger the unequal
99 sister chromatid exchange [20]. The frequency of rDNA recombination and ERC accumulation is
100 significantly reduced in a *fob1*Δ mutant due to loss of the fork block, thus extending RLS [18].
101 This rDNA-centric model of replicative aging has been modified over the years such that overall
102 rDNA instability, rather than ERC accumulation, is now considered the critical deleterious factor

103 toward lifespan [21]. Strains with virtually no ERC accumulation in old cells, but a high
104 frequency of rDNA recombination, are short-lived [22]. Also consistent with this idea, *sir2*Δ still
105 reduces RLS in a *fob1*Δ strain that has limited ERCs [23]. This raises several important
106 questions, including 1) does Sir2 regulate RLS through mechanisms independent of the rDNA,
107 and 2) how does rDNA instability shorten RLS? The experiments in this current study address
108 both of these questions.

109 As mentioned above, Sir2 is required for efficient cohesin association with the rDNA,
110 with stabilization of the tandem array a major mechanism for maintaining replicative longevity.
111 The cohesin complex in *S. cerevisiae* consists of four subunits, Mcd1/Scc1, Irr1/Scc3, Smc1, and
112 Smc3 [24]. The cohesin loading complex (Scc2/Scc4) deposits cohesin onto centromeres and
113 other sites across the chromosome arms (including rDNA) during S-phase to maintain sister
114 chromatid cohesion (SCC) until anaphase, when the Mcd1 subunit is cleaved by separase to
115 facilitate sister chromatid separation (reviewed in [24]). Cohesin defects result in chromosome
116 instability (CIN) and aneuploidy due to improper chromosome segregation during mitosis
117 (reviewed in [25]. Interestingly, cells lacking *SIR2* or heavily overexpressing *SIR2* have
118 increased rates of chromosome loss [26, 27]. Aneuploidy has been shown to shorten yeast RLS
119 by inducing proteotoxicity through improper expression levels [28]. Taken together, these results
120 suggest that Sir2 could impact RLS by regulating mitotic chromosome segregation during aging.

121 In this study, we investigated a potentially novel role for Sir2-limited yeast RLS through
122 maintenance of accurate chromosome segregation. In the process, we uncovered chromosome
123 instability and SCC defects in aging yeast cells that correlated with reduced levels of cohesin and
124 cohesin loader subunits. Forcibly manipulating Mcd1 subunit levels was sufficient to modify
125 RLS, suggesting a causative relationship to aging. Interestingly, cohesin association with

126 chromosome arms and the rDNA was generally reduced in old cells, but maintained or even
127 increased at centromeres, suggesting a programmed mechanism by which SCC is preferentially
128 maintained at centromeres to ensure cell viability. However, this comes at the expense of chronic
129 rDNA instability that is exacerbated by age-induced reductions in the RENT and
130 cohibin/monopolin complexes. Lastly, reducing rDNA instability by deleting *FOB1* suppressed
131 the general CIN phenotype in aged cells, leading to a model whereby rDNA instability caused by
132 cohesin depletion drives the defects in mitotic segregation of other chromosomes during
133 replicative aging.
134

135 **Results**

136 We previously reported a statistically significant overlap in genome-wide Sir2 binding sites
137 measured by ChIP-seq with cohesin binding sites measured by ChIP-Chip microarray analysis
138 [29, 30], consistent with the idea of a functional relationship between the two. Since deleting
139 *SIR2* reduced cohesin recruitment at individually selected loci [30], including the rDNA [31], we
140 decided to explore this result further using ChIP-Seq with exponentially growing WT and *sir2*Δ
141 strains in which the Mcd1 subunit of cohesin was C-terminally tagged with 13 copies of the myc
142 epitope (13xMyc). A composite plot of the sequencing data normalized to 1X read coverage
143 indicated both replicates of the *sir2*Δ strain exhibited dramatically reduced levels of Mcd1-myc
144 binding within the rDNA locus as compared to the WT strain (Fig 1A). This result was
145 confirmed with ChIP-qPCR using an IGS1 primer pair (Fig 1B) and supported earlier ChIP
146 results from the Nomura lab showing that cohesin recruitment to the rDNA requires Sir2 [31]. It
147 was also reported that cohesin released from the rDNA in a *sir2*Δ mutant preferentially
148 relocalized to pericentromeric regions as measured by fluorescence microscopy of GFP-tagged

149 Smc3 [32]. We attempted to recapitulate this result by creating a composite profile of all 16
150 centromeres but did not detect the same pericentromeric enrichment of Mcd1-myc in our *sir2*Δ
151 ChIP-seq datasets (Fig 1C). There was instead a trend toward reduced cohesion association.
152 Standard ChIP assays also did not reveal evidence of significant centromeric or pericentromeric
153 enrichment (Fig 1D). However, we cannot rule out the possibility that the ChIP signal was
154 diluted within an asynchronous cell population, compared to the microscopy data that examined
155 mitotic cells.
156
157 **Cohesin levels are depleted in old yeast cells**
158 Strains deleted for *SIR2* are short lived, but they likely do not fully recapitulate all
159 cellular changes that accompany normal replicative aging. We therefore hypothesized that more
160 severe effects of cohesin localization at centromeres could be uncovered by comparing
161 replicatively young vs. old cells in which Sir2 protein levels naturally declined. To isolate
162 sufficient quantities of old cells for ChIP assays we turned to Mother Enrichment Program
163 (MEP) strains developed by the Gottschling lab [33]. The aged cell purification procedure was
164 validated by increased bud scar staining with calcofluor white and by the expected reduction of
165 Sir2 protein (Fig 2A). The vacuolar protein Vma2, used as a loading control, does not deplete
166 with age [34], and detailed bud scar and protein quantitation from triplicate biological samples
167 are reported in S1 Fig. Since Sir2 is the catalytic subunit of both SIR and RENT (Fig 2B), it was
168 important to know which complexes were impacted by age. As shown in Figs 2C and 2D, Sir4
169 was depleted in old cells while Sir3 was not. Such a stark difference was considered highly
170 relevant because Sir2 and Sir4 tightly interact as a heterodimer that associates with the acetylated
171 H4 N-terminal tail [35]. Sir3 is subsequently recruited following H4K16 deacetylation to

172 complete SIR holocomplex formation on heterochromatin [36]. Myc-tagged Net1 (RENT
173 complex) was also depleted from old cells (Fig 2E), indicating that Sir2/Sir4 and the RENT
174 complex are both depleted during replicative aging, thus revealing a previously unrecognized
175 level of specificity in age-related Sir2 protein homeostasis. It should be noted that the Sir2
176 paralog, Hst1, which has the capacity to compensate for loss of Sir2, is also partially depleted
177 from old cells (S2A Fig).

178 Considering the depletion of multiple heterochromatin factors in old yeast cells and the
179 generally reduced Mcd1-myc ChIP signal in *sir2*Δ cells, we hypothesized that cohesin complex
180 levels may also drop in old cells. We attempted to individually myc-tag three different subunits
181 of cohesin (Mcd1, Smc1, and Irr1) in the MEP strain background. All cohesin subunits are
182 essential, and only two of the tagged proteins (Mcd1 and Smc1) were functional based on
183 recovery of viable cells and proper size on western blots. Both of these subunits were
184 significantly depleted in old cells (Fig 2F and S2B Fig), indicating the entire cohesion complex
185 was affected. Furthermore, a Myc-tagged Scc2 subunit of the Scc2/Scc4 cohesin loading
186 complex was age-depleted (S2C Fig), predicting that cohesion complex association with
187 chromatin should be generally sparse. ChIP assays for Mcd1-myc in aged cells did demonstrate
188 strong depletion from the rDNA intergenic spacer IGS1 as expected, but binding was
189 surprisingly enhanced at the centromere of chromosome IV (Fig 2G). Sir4-myc, on the other
190 hand, was depleted from *TELXV* in old cells (one of its normal targets) without shifting its
191 enrichment to centromeres (*CEN4*) or the rDNA (Fig 2H), indicating that not all age-depleted
192 proteins become enriched at centromeres. From these results we conclude that as cohesin is
193 depleted during replicative aging, a significant portion of the remaining complex is retained and
194 potentially redistributed to centromeres, consistent with an earlier finding that cohesin

195 preferentially associates with pericentromeric regions instead of chromosome arms when Mcd1
196 expression is artificially reduced below 30% of normal [37].
197
198 **Sister chromatid cohesion is compromised in old yeast cells**
199 SCC was surprisingly normal despite artificially reduced Mcd1 levels [37], leading us to
200 ask whether cohesion would be maintained in old yeast cells that were also depleted of cohesin.
201 To this end, we utilized strains with LacO arrays located approximately 10 kb away from
202 centromere IV (*CEN4*) or on the arm of chromosome IV at the *LYS4* locus located approximately
203 400 kb away from the centromere as proxy for arm cohesion [38, 39]. Differential positioning of
204 the array had no significant impact on RLS (S3 Fig). SCC was monitored by LacI-GFP
205 appearing either as one dot in the case of maintained cohesion or two dots in the case of cohesion
206 loss. Using an *mcd1-1* temperature sensitive mutant as a positive control [40], we observed a
207 significant increase in two dots when cells were synchronized in mitosis with nocodazole and
208 shifted to 37°C (Fig 3A and B). WT cells were next biotinylated and aged for 24 hours, followed
209 by purification with magnetic streptavidin beads. The maximum bud scar count was 13, which
210 was roughly half the maximum lifespan for this strain as measured by RLS assay. There was a
211 trend toward lost centromere and arm cohesion in old cells (>5 bud scars) when cultures were
212 synchronized in mitosis with nocodazole (Fig 3C, D, and E). When cells were not arrested with
213 nocodazole and only large budded (mitotic) cells were analyzed, significant cohesion loss was
214 observed in old mother cells compared to young (Fig 3E and F). Therefore, the limited amount of
215 cohesin complex remaining in old cells is functional, but has difficulty maintaining SCC when
216 microtubules are naturally allowed to exert pulling force on centromeres.
217

218 **Chromosome instability (CIN) increases during replicative aging**

219 Based on the cohesion defect in aged yeast cells, we next asked if they also display
220 elevated chromosome instability. Strains for this experiment have an artificial chromosome III
221 bearing a suppressor tRNA gene, *SUP11* [41]. Loss of the chromosome prevents suppression of
222 an ochre stop codon in *ADE2*, resulting in the classic *ade2* red colony phenotype. The frequency
223 of nondisjunction events was measured by counting half-sectored red/white colonies from young
224 and aged cell populations (Fig 4A). A *sir2*Δ mutant was included in the experiment because it
225 was previously reported to increase CIN [26], as was an *hst1*Δ mutant because of its potential for
226 functional overlap with Sir2 [42, 43]. Sectoring was elevated in young populations of *sir2*Δ and
227 *hst1*Δ mutants, and additively elevated in a *sir2*Δ *hst1*Δ double mutant (Fig 4B, left panel).
228 Interestingly, sectoring was even higher for aged populations of each strain, suggesting an
229 independent age-associated factor was involved. We next tested whether the *sir2*Δ effect on
230 sectoring was related to the pseudodiploid phenotype caused by derepression of the *HM* loci.
231 This reporter strain background was *MAT*α, so we deleted *HMR* (chrIII 293170-294330) to
232 eliminate the a1/a2 transcription factors, and then confirmed reversal of the pseudodiploid
233 phenotype by restoration of mating to the *sir2*Δ *hmr*Δ strains (data not shown). Importantly, this
234 procedure significantly suppressed sectoring of the young *sir2*Δ and *sir2*Δ *hst1*Δ mutants, but not
235 the *hst1*Δ mutant (Fig 4B, middle panel), indicating there was indeed a *sir2*Δ-induced
236 pseudodiploid effect that suppressed CIN (Fig 4B, middle panel). Aging increased sectoring in
237 each strain even when *HMR* was deleted, indicating the aging-associated CIN factor was
238 unrelated to mating type control.

239 Even though SCC was unaffected by forced cohesin depletion, rDNA array condensation
240 and stability were significantly impaired [37]. We therefore hypothesized that age-induced

241 chromosome instability could be related to rDNA instability caused by natural Sir2 and cohesin
242 depletion. To address this idea, *FOB1* was deleted to stabilize the rDNA and the sectoring
243 phenotype retested. As shown in Fig 4B (right panel), the age-associated increase in
244 chromosome instability for each mutant was generally reduced to that observed with young
245 *FOB1*$^{+}$ cells (Fig 4B, left panel), consistent with rDNA instability driving overall CIN.
246 What could be the mechanistic connection between the rDNA and centromeres? Previous
247 Hi-C analysis of the yeast genome and fluorescence microscopy of nucleolar proteins positioned
248 the rDNA off to one side of the nucleus, apparently secluded from the rest of the genome [44,
249 45]. The repetitive nature of rDNA precludes it from appearing in Hi-C contact maps, but closer
250 inspection of chromosome XII at 10 kb resolution indicated a clear interaction between unique
251 sequences flanking the centromere-proximal (left) edge of the array and *CEN12* (Fig 4C).
252 Further analysis of observed/expected contacts using HOMER revealed a looped structure
253 between the rDNA and *CEN12* (Fig 4D), which was recently reported to occur during anaphase
254 [46]. Interestingly, all centromeres in the yeast genome, including *CEN12*, cluster together in Hi-
255 C contact maps (Fig 4E; [44]), which by default also places them in contact with the left flank of
256 the rDNA. Taken together, these results suggest that the rDNA comes in close contact with
257 centromeres during mitosis, providing a potential window of time for rDNA instability to
258 physically impact the integrity of general chromosome segregation.
259
260 **Growth on galactose induces CIN and shortens RLS**
261 Since Sir2 and cohesin are both naturally depleted from replicatively aging yeast cells,
262 and mild Sir2 overexpression extends RLS [23], we hypothesized that manipulating cohesin
263 expression levels would also impact CIN and RLS. We initially attempted to overexpress the

264 Mcd1 subunit from a galactose inducible *GAL1* promoter and then measure minichromosome
265 loss frequency by counting ½ sectored colonies. However, simply growing the reporter strain in
266 galactose-containing media, even with an empty expression cassette, resulted in severe
267 minichromosome loss compared to glucose-containing media (Figs 5A and B). This effect was
268 specific to galactose, as growth with another non-preferred carbon source (raffinose) had no
269 effect on sectoring (Figs 5A and 5B). We next measured RLS with the minichromosome reporter
270 strain on YEP plates with 2% glucose, galactose, or raffinose. As shown in Fig 5C, galactose
271 decreased the mean RLS by ~50% compared to glucose (9.2 vs. 18.9 divisions), while raffinose
272 only marginally decreased lifespan to an average of 15.5 cell divisions. To confirm the galactose
273 effect on RLS was not specific to the minichromosome strain, RLS assays were repeated with the
274 well-characterized strains BY4741 (*MAT*a) and BY4742 (*MAT*α). Again, a significant decrease
275 in mean lifespan was observed for BY4741 (17.7 divisions) and BY4742 (18.9 divisions) on
276 galactose as compared to glucose (24.3 and 24.2 divisions, respectively) (Fig 5D), suggesting
277 that galactose triggers high rates of CIN through an unknown mechanism that also shortens RLS.
278

279 **RLS is modulated by Mcd1 expression levels**

280 To circumvent the use of galactose for *MCD1* overexpression we turned to an inducible
281 "Tet-On" promoter that is activated by doxycycline [47]. Strains harboring this integrated
282 cassette transcriptionally overexpressed *MCD1* approximately 7-fold compared to the empty
283 vector control (S4 Fig). *MCD1* was overexpressed in a "WT" strain (JH5275b) and a mutant
284 (JH5276b) containing an ochre stop codon in the *MCD1* open-reading frame (*mcd1L12STOP*)
285 that reduced Mcd1 protein levels to ~30% of normal [37]. With an empty pRS405 control vector
286 integrated, *mcd1L12STOP* exhibited a 40% reduction in mean RLS (9.9 divisions) compared to

287 WT (16.5 divisions), and overexpressing *MCD1* almost fully restored mean RLS to the mutant
288 (14.7 divisions) (Fig 6A). Especially intriguing was the observation that *MCD1* overexpression
289 extended mean RLS in the WT background to 19.6 division, an increase that was primarily due
290 to improved survival during the first ~15 divisions, followed by a steeper decline later (Fig 6A).
291 This biphasic pattern was highly reproducible, as it was observed in three independent RLS
292 experiments. Mechanistically, there could be a secondary age-related event at the RLS mid-point
293 that is beyond rescue by ectopic *MCD1* expression. Alternatively, doxycycline-induction could
294 eventually be attenuated due to the extended incubation times of RLS assays. Either way, the
295 results clearly indicate that similar to Sir2, the Mcd1 subunit of cohesin is a dosage-dependent
296 longevity factor.

297 Previous studies reported that Sir2 was required for efficient cohesin association with the
298 rDNA due to silencing of E-pro [16, 31], implying that Sir2 was upstream of cohesin. This
299 functional relationship could be more complex in the context of RLS, especially since both
300 factors are depleted with age. To explore further, we tested whether *SIR2* overexpression could
301 rescue the short RLS of an Mcd1-depleted *mcd1L12STOP* strain by integrating a second copy of
302 *SIR2* (2x*SIR2*) at the *LEU2* locus. As shown in Fig 6B, 2x*SIR2* partially rescued mean RLS of
303 the *mcd1L12STOP* strain (14.1 versus 9.9 divisions), and also increased maximum RLS of the
304 WT strain as expected. Reciprocally, we asked whether *MCD1* overexpression could suppress
305 the short RLS of a *sir2*Δ *hst1*Δ mutant. The double mutant was chosen to avoid any redundancy
306 between the two sirtuins. Mean RLS was clearly not increased by *MCD1* overexpression as
307 compared to empty vector (10.1 versus 9.7 divisions, Fig 6C), confirming that *SIR2* was
308 upstream of *MCD1* in regulating RLS.

309 Considering the strong depletion of cohesin from rDNA in old cells (Fig 2G), and
310 extended RLS when *MCD1* was overexpressed (Fig 6A), we next tested whether aging-induced
311 rDNA instability was suppressed by *MCD1* overexpression using a reporter strain harboring
312 *ADE2* in the rDNA array [23]. There was a large increase of red/white sectoring (marker loss) in
313 old cells that was suppressed upon *MCD1* overexpression (Fig 6D). In the absence of *SIR2*,
314 however, red/white sectoring was high in both young and old cells when the empty vector
315 (pRF10) was integrated, and *MCD1* overexpression did not significantly reduce rDNA instability
316 in either population (Fig 6D), indicating that at least some Sir2 was required for Mcd1 to impact
317 rDNA stability. We conclude that loss of Sir2 and cohesin in aging cells causes rDNA array
318 instability that exacerbates CIN.
319

320 **RLS extension by CR correlates with improved chromosome stability**

321 Reducing glucose concentration in the growth medium is effective at extending RLS and
322 is considered a form of caloric restriction (CR) for yeast [48, 49]. There have been several
323 hypotheses put forth for the underlying mechanisms, including stabilization of the rDNA [21].
324 Since *MCD1* overexpression suppressed rDNA recombination and extended RLS, we
325 hypothesized that CR would suppress the shortened RLS of a cohesion-depleted *mcd1L12STOP*
326 mutant strain. Indeed, CR extended RLS of both the WT and *mcd1L12STOP* strains (Fig 7A).
327 However, the suppression was apparently not due to maintenance of global cohesion levels
328 because steady state Mcd1-13xMyc was still depleted in restricted old cells (Fig 7B). CR also
329 strongly suppressed minichromosome loss in young and aged cells, even in the *sir2*Δ *hst1*Δ
330 double mutant (Fig 7C). Importantly, this CR effect also correlated with almost complete rescue
331 of RLS for the *sir2*Δ *hst1*Δ mutant (Fig 7D). Taken together, the results reveal a new mechanism

332 for RLS extension by CR, whereby stabilization of the rDNA locus helps maintain general
333 mitotic chromosome stability to protect against aneuploidy.
334

335 ## Discussion

336 **Nuclear protein depletion during replicative aging as a paradigm for aging pathologies**

337 During this study the majority of chromatin-associated proteins analyzed by western
338 blotting were depleted in replicatively aged yeast cells. The only protein unaffected by age, other
339 than the vacuolar Vma2 control, was Sir3. A similar proportion of homologous recombination
340 proteins were depleted in an independent analysis of old cells, with Rad52 the only one not
341 affected [50]. These results indicate there is at least some selectivity to the depletion of nuclear
342 proteins in old cells. However, the large number of depleted factors also makes it likely that
343 targeted nuclear protein deficiency could lead to multiple age-associated phenotypes.
344 Replicatively aging yeast cells appear especially susceptible to this phenomenon, as even total
345 core histone levels are depleted [51]. Evidence also exists for histone depletion during aging of
346 metazoan organisms, including mammals (reviewed in [52]). More generally, global protein
347 turnover is elevated in cells from prematurely aging progeria patients, which may trigger higher
348 translation rates [53]. This is significant because reducing translation is a means of extending
349 lifespan in multiple organisms [54]. Ribosomal proteins appear to accumulate in old cells [55],
350 again consistent with protein synthesis being a driver of aging [56]. The mechanism(s) driving
351 nuclear protein depletion in old yeast mother cells remain unclear.

352 The specificity for Sir2/Sir4 depletion over Sir3 is intriguing given that Sir2 and Sir4
353 form a tight complex that allosterically stimulates the deacetylase activity of Sir2 [57]. Sir2/Sir4
354 also binds to H4K16-acetylated chromatin independent of Sir3, which is subsequently recruited

355 to complete the SIR holocomplex once H4K16 is deacetylated [36]. The mechanism for Sir2/Sir4
356 depletion from old cells remains uncharacterized, though in non-aging cell populations the
357 stability/turnover of Sir4, but not Sir2, is mediated by the E3 ubiquitin ligase San1 [58], which
358 has also been implicated as a quality control E3 ligase for mutated/unfolded nuclear proteins
359 [59]. Whether San1 controls Sir4 stability during aging remains unknown, but since Sir4 is more
360 severely depleted than Sir2 in old cells (Figs 2A and 2C), Sir4 could be selectively depleted from
361 the SIR complex, thus leaving Sir2 unprotected and then subject to turnover through a different
362 mechanism. Alternatively, Sir2/Sir4 could be equally depleted as a complex from telomeres and
363 the *HM* loci (not necessarily via San1), leaving the nucleolar pool of Sir2/RENT as more
364 resistant to aging. Under this scenario, protecting the integrity of the rDNA array could take
365 precedence over other heterochromatic domains. Interestingly, the *Schizosaccharomyces pombe*
366 San1 ortholog has also been implicated in a chaperone-assisted degradation pathway that
367 functions in quality control of kinetochores to promote chromosome stability [60].
368 Sir2 depletion in replicatively aged yeast cells is reminiscent of Sirt1 depletion in serially
369 passaged mouse embryonic fibroblasts (MEFs), which correlates with declining mitotic activity
370 [61]. Sir2 and Sirt1 are both known to function in regulating DNA replication origins [62, 63],
371 and the effect of deleting *SIR2* on early origin firing is thought to be mediated by competition for
372 limiting factors with the repeated rDNA origins [64]. Furthermore, CR has been proposed to
373 extend RLS by reducing rDNA origin firing, which improves overall genome replication [65].
374 Therefore, depleted cohesin in old cells could potentially cause rDNA instability by impacting
375 DNA replication.
376
377 **A precarious balance between rDNA and centromeric cohesion**

378 Sister chromatid cohesion (SCC) ensures chromosomes are not segregated until the
379 Mcd1/Scc1 cohesin subunit is cleaved in response to a mitotic spindle checkpoint signal that all
380 chromosomes are properly attached to microtubules and aligned at the metaphase plate (reviewed
381 in [24]). Cohesin is also critical during meiosis, and it is well established in mammals that SCC
382 defects occur in the oocytes of older mothers, causing meiotic chromosome missegregation
383 events during both anaphase I and II [66]. This phenomenon is believed to be a major
384 mechanism for increased aneuploidy risk that usually results in embryonic lethality, or in the
385 case of chromosome 21 trisomy, Down's syndrome in children. The meiotic cohesin subunit
386 Rec8 is depleted in the oocytes of older mice, as is Shugoshin (Sgo2), which normally
387 protects/maintains centromeric cohesin [67]. More recent experiments in *Drosophila* suggest that
388 oxidative stress in aged oocytes contributes to the SCC defects [68]. Our results in replicatively
389 aging yeast cells reveal that aging-induced cohesin depletion and the resulting chromosome
390 missegregation can extend to mitotic cells. Though cohesin depletion or defects have not been
391 reported for mammalian somatic cells, the mitotic spindle checkpoint protein BubR1 is depleted
392 in dynamic somatic tissues such as spleen [69]. Deficiency of this protein results in premature
393 aging phenotypes [69], while overexpression extends lifespan [70]. This is similar to the effects
394 we observe with Mcd1 depletion and overexpression on yeast RLS. Interestingly, BubR1 is also
395 a deacetylation target of Sirt2, which appears to stabilize the protein and extend lifespan, thus
396 linking mitotic spindle checkpoint regulation to NAD^+ metabolism [71]. It remains unclear if
397 Sir2, Hst1, or other sirtuins regulate the yeast BubR1 ortholog, Mad3, or additional checkpoint
398 and kinetochore proteins.
399 SCC is the canonical function for cohesin, though the complex also functions in
400 establishing and regulating genome organization at the level of chromatin structure, gene

401 regulation, and double strand break (DSB) repair (reviewed in [72]). Among these various
402 processes, SCC at centromeres appears the most critical because artificial depletion of Mcd1 to
403 <30% of normal levels results in preferential cohesin binding to pericentromeric regions rather
404 than cohesin associated regions (CARs) on chromosome arms [37]. SCC was also well
405 maintained in these strains at the expense of normal chromosome condensation, DNA repair, and
406 rDNA stability [37]. In aged yeast cells we observed relative enrichment of Mcd1-myc at
407 centromeres as compared to loss at the rDNA (IGS1) locus (Fig 2G), suggesting an attempt by
408 cells to maintain centromere cohesion at all costs, similar to what occurred in the artificially
409 depleted system. Despite maintaining the cohesin complex at centromeres, SCC was still
410 impaired in the older cells, especially when tension was maintained. In contrast, an independent
411 study that analyzed significantly older mother cells (~20 generations) than in our study (~6
412 generations) observed reduced cohesin enrichment at centromeres [50]. Collectively, the results
413 suggest that centromere-associated cohesin is preferentially retained during the initial stages of
414 replicative aging, but then eventually breaks down below a critical threshold in the oldest cells.
415 Numerous nuclear proteins are depleted in old yeast cells, not just cohesin subunits, so
416 we hypothesize that defects in other nuclear processes mediated by such factors also contribute
417 to SCC defects and chromosome instability either directly or indirectly. The depleted cohesin
418 loading complex (Scc2/4) is an obvious candidate due to its role in loading cohesin onto
419 chromatin. Similarly, the depleted Lrs4/Csm1(cohibin complex) is proposed to act as a cohesin
420 clamp onto rDNA chromatin [73], and also functions at centromeres to maintain mitotic integrity
421 [74]. Sir2 and Hst1 are also obvious candidates given the earlier finding that H4K16
422 deacetylation at centromeres by Sir2 helps maintain chromosome stability [26]. Hst1 also binds
423 centromeric DNA *in vitro* and *in vivo* [75], though the functional relevance of that association

424 remains uncharacterized. The suppression of age-associated mini-chromosome loss in the
425 absence of *FOB1* clearly points to rDNA instability as an unexpected source of general CIN.
426 Such a relationship is reinforced by the observed depletion of nucleolar proteins Net1 and Lrs4
427 in old cells (Figs 2E and S2D), both of which are required for normal rDNA/nucleolar integrity
428 and stable cohesin association with the rDNA [14, 73, 76].

429 How could destabilization of the rDNA locus result in general chromosome instability
430 and shortened RLS? As depicted in Fig 4, unique sequence flanking the rDNA on chromosome
431 XII contacts the centromere of each chromosome, including XII. Whether the actual rDNA genes
432 contact centromeres remains unclear due to the limitations of Hi-C analysis with repetitive DNA.
433 However, specific regions of the rDNA were previously shown to associate with various non-
434 rDNA chromosomal regions using an anchored 4C approach [77]. Loss of cohesin from the
435 rDNA could potentially disrupt long-range interactions with centromeres or non-centromeric
436 regions of cohesin association that influence chromosome integrity. One potential mechanism
437 could be significant disruption of overall chromosome condensation during mitosis, as the
438 cohesin appears to play the major role in chromosome condensation in budding yeast instead of
439 the condensin complex [46], which is different from metazoan organisms where condensin is the
440 primary condensation machinery.

441 Interestingly, another class of nuclear factors depleted in old yeast cells are several DNA
442 repair proteins [50]. Consequently, the lack of proper DNA repair while the rDNA becomes
443 destabilized correlates with fragmentation of chromosome XII and the other chromosomes, with
444 rDNA sequences actually being transferred into the other chromosomes. It was proposed that
445 accumulation of breaks and rearrangements ultimately causes cell death during replicative aging.
446 Such cells were significantly older (>25 divisions) compared to the cells in our study, which

447 averaged 5-6 divisions. Alternatively, it is possible that these presumably random
448 rearrangements disrupt normal SCC, leading to CIN.
449
450 **Aneuploidy as an aging mechanism**
451 All 16 *S. cerevisiae* chromosomes harbor essential genes, so if a single chromosome is
452 lost from a haploid yeast cell, then the affected mother or daughter cell should become inviable
453 and no longer divide. Given the elevated frequency of chromosome loss during replicative aging,
454 the chances of generating an inviable mother cell during a replicative aging assay increases after
455 each subsequent division. Therefore, at least a portion of the replicative lifespan in haploid yeast
456 cells is controlled by the ability to maintain all 16 chromosomes. Complete loss of a
457 chromosome would not be an immediate viability issue for diploid cells, however, as the chances
458 of losing both homologs in a single mitosis are exceedingly rare. On the other hand, haploid
459 strains that are disomic for individual chromosomes are often short lived, with longer
460 chromosomes typically having larger effects [28]. It was hypothesized that such strains suffer
461 from proteotoxic stress due to inappropriate protein expression levels. Therefore, a similar
462 mechanism could shorten RLS in a diploid strain that is trisomic for an individual chromosome,
463 though this has not yet been tested. Aneuploidy is also a hallmark of aging in the germline [78],
464 and somatic tissues of mammals [70, 79], making it a conserved feature of aging from yeast to
465 humans.
466 Another exciting feature of this study is the suppression of CIN by CR growth conditions
467 that extend RLS. This effect was independent of the reduced cohesin levels in aged cells, and
468 even improved RLS of the cohesin-depleted strains. Since SCC is normal in the cohesin-depleted
469 strain [37], we hypothesize that CR reinforces other processes that are defective due to reduced

470 cohesin or other depleted factors that promote rDNA stability. Indeed, CR is known to suppress
471 rDNA instability in yeast cells [80, 81], and improve overall genome replication efficiency [65].
472 Hi-C analysis also suggests there could be direct effects of rDNA structure on centromere
473 function, which will be the focus of future investigation.
474

475 # Methods

476 **Yeast strains, plasmids, and media**

477 Yeast strains were primarily grown at 30°C in Yeast Peptone Dextrose (YPD) or
478 Synthetic Complete (SC) medium for strains bearing plasmids [82]. *SIR2, HST1*, or *FOB1* open
479 reading frames were disrupted with one-step PCR-mediated gene replacement using *kanMX4*,
480 *natMX4*, or *hphMX4* drug resistance markers, respectively. The *HMR* deletion by replacement
481 with *hphMX4* spans sacCer3 genome coordinates of chrIII 293170-294330. All C-terminally
482 13xMyc (EQKLISEEDL) tagged proteins were fused at the endogenous loci of haploid MEP
483 strains UCC5181 and UCC5179, followed by crossing to generate homozygous diploids. All
484 deletions and fusions were confirmed by colony PCR, western blotting, or both. pRF4 was
485 constructed by PCR amplifying the *MCD1* open reading frame from ML1 genomic DNA and
486 ligating into *Pst*I and *Not*I sites of pCM252, a tetracycline/doxycycline inducible overexpression
487 vector available from Euroscarf (http://www.euroscarf.de). pRF10 and pRF11 were constructed
488 by removing the expression cassette by *Pvu*II blunt end digestion of pCM252 and pRF4,
489 respectively, and ligating it between the *Pvu*II sites of pRS405 bearing the *LEU2*, thus replacing
490 the *TRP1* marker with *LEU2*. pSB760 and pSB766 are integrating and *2μ LEU2* vectors,
491 respectively, bearing a single copy of *SIR2* [83]. All strains used in this work are listed in S1
492 Table and all primers are listed in S2 Table.

493

494 **Old yeast cell isolation**

495 Old yeast cell enrichment was based on MEP (Mother Enrichment Program) strains [33,
496 34]. For all assays, 1 µL of stationary phase culture was inoculated into 100 mL of YPD medium
497 and then grown into log phase. Approximately $1x10^8$ cells were harvested, and centrifuged cell
498 pellets washed 3 times with 1x phosphate buffered saline (PBS). Cells were then resuspended in
499 1 mL of PBS and mixed with 5 mg of Sulfo-NHS-LC-Biotin (Pierce) per $1x10^8$ cells for 30
500 minutes at room temperature. After biotin labeling, $5x10^7$ cells were added to 1.5 L YPD cultures
501 containing 1µM estradiol, and 100 µg/mL ampicillin to prevent bacterial contamination. These
502 cultures were allowed to grow for 24 hours before being processed in a downstream assay
503 specific manner (see below). For non-MEP strain backgrounds, estradiol was not added to the
504 cultures.

505

506 **Old cell western blots**

507 Two large scale cultures (1.5 L) were used for each western blot experiment
508 corresponding to approximately $2x10^7$ total old cells after purification. Cells were pelleted using
509 a Sorvall RC-5B Plus centrifuge with an SLA-3000 rotor at 2000 rpm, and then resuspended at a
510 density of $6x10^8$ cells/mL in RNAlater (Ambion) for 45 minutes in two separate conical tubes.
511 Following fixation, cells were pelleted and resuspended in 45 mL of cold 1xPBS, 2 mM EDTA
512 in 50 mL conical tubes. The mixture was incubated at 4°C for 30 min with 800 µL of
513 Streptavidin MicroBeads (Miltenyi Biotec), which were then purified through an autoMACS Pro
514 Cell Separator using the posseld2 program (UVA flow cytometry core facility). A 20 µL aliquot
515 of each output was used for bud scar counting using calcofluor white staining, before combining

516 the isolated samples into a single microfuge tube. Samples were frozen at -80°C before protein
517 extraction. Thawed cells were vortexed twice for 1 min in 20% TCA (trichloroacetic acid) with
518 ~100 µL of acid washed glass beads with a brief cooling period in between vortexing. Beads
519 were allowed to settle before removing the supernatant to a fresh microfuge tube. A 250 µL wash
520 of 5% TCA was applied twice to the beads and pooled with the initial lysis sample. Proteins were
521 precipitated at 10,000 rpm in a microfuge for 5 min at 4°C. The pellets were resuspended in 50
522 µL of 1x SDS sample buffer (50 mM Tris-HCl pH 6.8, 2% SDS, 10% Glycerol, 3.6 M 2-
523 mercaptoethanol) and neutralized with 30 µL of 1M Tris-HCl, pH 8.0. Samples were run on a
524 9% (w/v) SDS-polyacrylamide gel and transferred to an Immobilon-P membrane (Millipore).
525 Membranes were incubated for 1 hour at room temperature in 1xTBST + 5% non-fat milk with
526 primary antibodies (1:2000 α-Myc 9E10, 1:5000; α-Vma2 (Life Technologies); 1:5000 α-Sir2
527 (Santa Cruz Biotechnology); 1:1000 α-Sir4 (Santa Cruz Biotechnology); 1:1000 α-Sir3 (Santa
528 Cruz Biotechnology). HRP-conjugated secondary antibodies (Promega) were diluted 1:5000, and
529 detected using chemiluminescence with HyGLO (Denville Scientific).
530
531 **ChIP Assays with old and young cells populations**
532 Two 1.5 L cultures were used for each biological replicate sample. After centrifugation,
533 cells were washed with 1xPBS and resuspended in 45 mL of 1xPBS and incubated with 800 µL
534 of streptavidin microbeads, followed by sorting with the autoMACS Pro Cell Separator. Sorted
535 cells were immediately crosslinked with 1% formaldehyde for 20 min at room temperature, then
536 transferred to screw cap microcentrifuge tubes and the pellets flash frozen in liquid nitrogen.
537 Cells were thawed and lysed in 600 µL FA140 Lysis buffer (50 mM HEPES, 140 mM NaCl, 1%
538 Triton X-100, 1 mM EDTA, 0.1% SDS, 0.1 mM PMSF, 1x protease inhibitor cocktail; Sigma)

539 by shaking with acid-washed glass beads in a Mini-Bead beater (Biospec Products). Cell lysates
540 were recovered and sonicated for 30 cycles of 30 sec "on" and 30 sec "off" in a Diagenode
541 Bioruptor followed by centrifugation at 16,000 x g. A 1/10th supernatant volume input was taken
542 for each sample and crosslinking reversed by incubating overnight at 65°C in 150 µL elution
543 buffer (TE, 1% SDS). The remaining supernatant was used for immunoprecipitation overnight at
544 4°C with 5 µg of primary antibody and 30 µL of protein G magnetic beads (Pierce), followed by
545 washing 1x with FA-140 buffer, 2x with FA-500 buffer (FA-140 with 500 mM NaCl), and 2x
546 with LiCl solution (10 mM Tris-HCl, pH 8.0, 250 mM LiCl, 0.5% NP-40, 0.5% SDS, 1 mM
547 EDTA). DNA was eluted twice with 75 µL of elution buffer in a 65°C water bath for 15 min.
548 The eluates were combined and crosslinking reversed. Input and ChIP DNA samples were
549 purified by an Invitrogen PureLink™ PCR purification kit. Finally, ChIP DNA was quantified by
550 real-time PCR and normalized to the input DNA signal. Young cells were collected from flow
551 through out of the autoMACS cell sorter and then processed as described for the aged cells. For
552 ChIP assays on unsorted populations, cells were grown to log phase in 100 mL YPD before
553 formaldehyde cross-linking for 20 min at 30°C while shaking. Additionally, 2.5 mg of protein
554 was used for the IP instead of the entire lysate, and the chromatin solution was sonicated for 50
555 cycles rather than 30.
556
557 **ChIP-Seq Library Preparation**
558 Chromatin was prepared in a similar manner to old cell ChIP assays with the following
559 exceptions. Cells were grown to log phase in 200 mL YPD and fixed for 20 min with 1%
560 formaldehyde. Lysate volumes were adjusted to 4 mL in FA-140 lysis buffer and sonicated 5
561 times with a Branson 250 Digital Sonifier for 30 sec at 70% amplitude. Samples were cooled on

562 ice for at least 1 min between sonication periods. The lysate was split into 3 microcentrifuge
563 tubes and spun for 10 min at 10,000 rpm in a microfuge at 4°C. The entire supernatant from 1
564 tube was used for immunoprecipitation overnight with 15 μg of α-Myc 9E10 antibody and 30 μL
565 of protein G magnetic beads (Pierce). After washing, elution, and reverse cross-linking, 100 mg
566 of Proteinase K was added for 2 hr at 42°C. Chromatin was purified in a Zymogen DNA Clean
567 and Concentrator-5 Kit and quantified using a Qubit fluorometric device. A minimum of 20 ng
568 of DNA was used as input for NEBNext® library construction. ML150 libraries were sequenced
569 on an Illumina Nextseq and ML163 libraries on an Illumina Miseq by the UVA Genome
570 Analysis and Technology Core. Sequencing files are available at GEO accession number
571 GSE117037. Sequencing reads were mapped to the sacCer3 genome using bowtie2 with default
572 settings. Corresponding bam files were further processed to produce the coverage plots shown in
573 Fig 1 with the Deeptools package of Galaxy (https://usegalaxy.org/).
574

575 **Sister chromatid cohesion assay**

576 From 50 mL log phase SC cultures of strains 3349-1B, 3312-7A, and 3460-2A, $5x10^7$
577 cells were washed and biotinylated as described in the Old Cell Isolation section. This population
578 was transferred into a 1.5 L SC culture and allowed to grow for 12 hr. The original biotinylated
579 population was then purified by incubation with 300 μL of streptavidin micro beads followed by
580 gravity filtration through a Miltenyi LS column. The column was washed twice with 5 ml of PBS
581 and the enriched cell/bead population was aged for an additional 12 hr in a fresh 1.5 L SC culture
582 before being purified for a second time with an additional 200 μL of beads. Eluted cells (still
583 bound to beads) were processed as described below for young cells.

584 From the original log phase culture, $5x10^7$ cells were arrested in a fresh 50 mL SC culture
585 containing 10 µg/mL nocodazole for 1.5 hr. For the *mcd1-1* strain 3312-7A, cells were also
586 shifted to 36°C at this time. Bud scars were stained with the addition of 1 mL of supernatant
587 from a solution of PBS and 5 mg of Calcofluor white that was centrifuged to eliminate
588 aggregates. Non-arrested cells were directly stained with calcofluor. Cells were then pelleted and
589 washed in PBS. Following staining, 200 µL of 4% paraformaldehyde was added directly to the
590 cell pellet and allowed to crosslink for 15 min at room temperature. The cell pellet was washed
591 once with PBS and resuspended in ~100-200 µL of 0.1 $MKPO_4$/1 M sorbitol, pH 6.5. Images
592 were captured with a Zeiss Axio Observer z1 widefield microscope using a 64x oil objective
593 lens.
594
595 **Replicative lifespan assays**
596 Lifespan assays were carried out essentially the same as previously described [84].
597 Briefly, small aliquots of log phase cultures were dripped in a straight line onto solid agar YPD
598 with 2% glucose. From the initial populations, a minimum of 32 virgin daughter cells were
599 picked for lifespan assays with daughter cells being selectively pulled away from mother cells
600 using a fiberoptic dissection needle and on a Nikon Eclipse 400 microscope. All virgin daughters
601 were required to bud at least one time to be included in the experiment and dissection was
602 carried out over the course of several days with temporary incubation at 4°C in between
603 dissection periods to stop division. Cells were considered dead when they stopped dividing for a
604 minimum of 2 generation times (180 min).
605
606 **Chromosome loss (sectoring) assay**

607 The colony sectoring assay was performed on SC plates with adenine limited to 80 μM.
608 Frequency of mini-chromosome loss represents the number of ½ or ¼ red/white sectored
609 colonies divided by the sum of sectored and white colonies. Cells were plated to an approximate
610 density of 500 cells/plate based on counts from a Brightline hemacytometer. Any plates bearing
611 greater than 1000 cells were discarded. Three biological replicates of each strain were
612 performed, with at least 10 plates counted per replicate. For old cell populations, ~$5x10^6$
613 biotinylated cells were aged in 1.5 L of YPD for 24 hr. Cells were incubated with 300 μL of
614 streptavidin magnetic beads (New England Biolabs) and manually washed 4 times with PBS on a
615 magnetic stand, then plated onto the limiting adenine SC plates such that ~500 colonies
616 appeared. Bud scars were not counted because the size of the beads prohibited visualization.
617

618 **RT-qPCR measurement of *MCD1* overexpression**

619 Doxycycline was added to log phase cultures at a concentration of 2 μg/mL for 6 hr in
620 order to induce expression of MCD1 from pRF4. Total RNA was extracted using a standard acid
621 phenol extraction protocol [85]. cDNA was created from ~1 μg of RNA using a Verso cDNA
622 synthesis kit (Thermo Fisher). *MCD1* expression levels were quantified on an Applied
623 Biosystems StepOne real time PCR machine with primers JS2844 and JS2949, and normalized to
624 actin transcript levels (primers JS1146 and JS1147).
625

626 **Hi-C analysis**

627 Log-phase cultures were cross-linked with 3% formaldehyde for 20 min and quenched
628 with a 2x volume of 2.5M Glycine. Cell pellets were washed with dH_2O and stored at -80°C.
629 Thawed cells were resuspended in 5 ml of 1X NEB2 restriction enzyme buffer (New England

630 Biolabs) and poured into a pre-chilled mortar containing liquid N_2. Nitrogen grinding was
631 performed twice as previously described [86], and the lysates were then diluted to an OD_{600} of 12
632 in 1x NEB2 buffer. 500 µl of cell lysate was used for each Hi-C library as follows. Lysates were
633 solubilized by the addition of 50 µl 1% SDS and incubation at 65°C for 10 min. 55 µl of 10%
634 TritonX-100 was added to quench the SDS, followed by 10 µl of 10X NEB2 buffer and 15 µl of
635 *Hin*dIII (New England Biolabs, 20 U/µl) to digest at 37°C for 2 hr. An additional 10 µl of
636 *Hin*dIII was added for digestion overnight. The remainder of the protocol was based on
637 previously published work with minor exceptions [87], see supplemental experimental
638 procedures for details. Hi-C sequencing libraries were prepared with reagents from an Illumina
639 Nextera Mate Pair Kit (FC-132-1001) using the standard Illumina protocol of End Repair, A-
640 tailing, Adapter Ligation, and 12 cycles of PCR. PCR products were size selected and purified
641 with AMPure XP beads before sequencing with an Illumina Miseq or Hiseq.
642

643 **Author Contributions**

644 Conceptualization; R.D.F. and J.S.S.; Methodology, R.D.F., M.L. and J.S.S.; Software, R.D.F.;
645 Strain Creation and Validation, R.D.F., N.M., E.F., and M.L.; Plasmid Creation and Validation,
646 R.D.F., E.F., and M.L; Formal Analysis, R.D.F.; Data Curation, R.D.F.; Writing-Original Draft,
647 R.D.F. and J.S.S.; Writing Review & Editing, R.D.F., M.L., and J.S.S; Supervision, J.S.S.;
648 Project Administration, J.S.S.; Funding Acquisition, J.S.S.
649

650 **Acknowledgments**

651 We thank Dan Gottschling and all lab members for kindly providing yeast strains and initial
652 advice on using the MEP system. Stefan Bekiranov, Job Dekker, Jon Belton, Maitreya Dunham,

653 Ivan Liachko, Maxim Imakev, and Anton Goloborodko all provided valuable advice on Hi-C
654 protocols and analysis methods. We thank Doug Koshland for providing the Mcd1 reduction and
655 cohesion assay strains, and Matt Kaeberlein for rDNA marker loss strains. Special thanks to
656 Todd Stukenberg for microscopy assistance. Lastly, thanks to David Auble for critically reading
657 the manuscript and providing comments prior to submission. We declare no conflicts of interest.
658

659 **References**

660 1. Mortimer RK, Johnston JR. Life span of individual yeast cells. Nature.
661 1959;183(4677):1751-2. PMID: 13666896.
662 2. Wasko BM, Kaeberlein M. Yeast replicative aging: a paradigm for defining conserved
663 longevity interventions. FEMS Yeast Res. 2014;14(1):148-59. PMID: 24119093.
664 3. Buck SW, Gallo CM, Smith JS. Diversity in the Sir2 family of protein deacetylases. J
665 Leukoc Biol. 2004;75(6):939-50. PMID: 14742637.
666 4. Gomes AP, Price NL, Ling AJ, Moslehi JJ, Montgomery MK, Rajman L, et al. Declining
667 NAD^+ induces a pseudohypoxic state disrupting nuclear-mitochondrial communication during
668 aging. Cell. 2013;155(7):1624-38. PMID: 24360282.
669 5. Brachmann CB, Sherman JM, Devine SE, Cameron EE, Pillus L, Boeke JD. The *SIR2*
670 gene family, conserved from bacteria to humans, functions in silencing, cell cycle progression,
671 and chromosome stability. Genes Dev. 1995;9(23):2888-902. PMID: 7498786.
672 6. Rine J, Herskowitz I. Four genes responsible for a position effect on expression from
673 *HML* and *HMR* in *Saccharomyces cerevisiae*. Genetics. 1987;116(1):9-22. PMID: 3297920.
674 7. Gartenberg MR, Smith JS. The nuts and bolts of transcriptionally silent chromatin in
675 *Saccharomyces cerevisiae*. Genetics. 2016;203(4):1563-99. PMID: 27516616.

676 8. Dang W, Steffen KK, Perry R, Dorsey JA, Johnson FB, Shilatifard A, et al. Histone H4
677 lysine 16 acetylation regulates cellular lifespan. Nature. 2009;459(7248):802-7. PMID:
678 19516333.
679 9. Smeal T, Claus J, Kennedy B, Cole F, Guarente L. Loss of transcriptional silencing
680 causes sterility in old mother cells of *S. cerevisiae*. Cell. 1996;84(4):633-42. PMID: 8598049.
681 10. Schlissel G, Krzyzanowski MK, Caudron F, Barral Y, Rine J. Aggregation of the Whi3
682 protein, not loss of heterochromatin, causes sterility in old yeast cells. Science.
683 2017;355(6330):1184-7. PMID: 28302853.
684 11. Bryk M, Banerjee M, Murphy M, Knudsen KE, Garfinkel DJ, Curcio MJ. Transcriptional
685 silencing of Ty1 elements in the *RDN1* locus of yeast. Genes Dev. 1997;11(2):255-69. PMID:
686 9009207.
687 12. Smith JS, Boeke JD. An unusual form of transcriptional silencing in yeast ribosomal
688 DNA. Genes Dev. 1997;11(2):241-54. PMID: 9009206.
689 13. Shou W, Seol JH, Shevchenko A, Baskerville C, Moazed D, Chen ZW, et al. Exit from
690 mitosis is triggered by Tem1-dependent release of the protein phosphatase Cdc14 from nucleolar
691 RENT complex. Cell. 1999;97(2):233-44. PMID: 10219244.
692 14. Straight AF, Shou W, Dowd GJ, Turck CW, Deshaies RJ, Johnson AD, et al. Net1, a
693 Sir2-associated nucleolar protein required for rDNA silencing and nucleolar integrity. Cell.
694 1999;97(2):245-56. PMID: 10219245.
695 15. Li C, Mueller JE, Bryk M. Sir2 represses endogenous polymerase II transcription units in
696 the ribosomal DNA nontranscribed spacer. Mol Biol Cell. 2006;17(9):3848-59. PMID:
697 16807355.

698 16. Kobayashi T, Ganley AR. Recombination regulation by transcription-induced cohesin
699 dissociation in rDNA repeats. Science. 2005;309(5740):1581-4. PMID: 16141077.
700 17. Sinclair DA, Guarente L. Extrachromosomal rDNA circles--a cause of aging in yeast.
701 Cell. 1997;91(7):1033-42. PMID: 9428525.
702 18. Defossez PA, Prusty R, Kaeberlein M, Lin SJ, Ferrigno P, Silver PA, et al. Elimination of
703 replication block protein Fob1 extends the life span of yeast mother cells. Mol Cell.
704 1999;3(4):447-55. PMID: 10230397.
705 19. Kobayashi T, Horiuchi T. A yeast gene product, Fob1 protein, required for both
706 replication fork blocking and recombinational hotspot activities. Genes Cells. 1996;1(5):465-74.
707 PMID: 9078378.
708 20. Takeuchi Y, Horiuchi T, Kobayashi T. Transcription-dependent recombination and the
709 role of fork collision in yeast rDNA. Genes Dev. 2003;17(12):1497-506. PMID: 12783853.
710 21. Ganley AR, Kobayashi T. Ribosomal DNA and cellular senescence: new evidence
711 supporting the connection between rDNA and aging. FEMS Yeast Res. 2014;14(1):49-59.
712 PMID: 24373458.
713 22. Ganley AR, Ide S, Saka K, Kobayashi T. The effect of replication initiation on gene
714 amplification in the rDNA and its relationship to aging. Mol Cell. 2009;35(5):683-93. PMID:
715 19748361.
716 23. Kaeberlein M, McVey M, Guarente L. The SIR2/3/4 complex and SIR2 alone promote
717 longevity in *Saccharomyces cerevisiae* by two different mechanisms. Genes Dev.
718 1999;13(19):2570-80. PMID: 10521401.
719 24. Marston AL. Chromosome segregation in budding yeast: sister chromatid cohesion and
720 related mechanisms. Genetics. 2014;196(1):31-63. PMID: 24395824.

721 25. Wood AJ, Severson AF, Meyer BJ. Condensin and cohesin complexity: the expanding
722 repertoire of functions. Nat Rev Genet. 2010;11(6):391-404. PMID: 20442714.
723 26. Choy JS, Acuna R, Au WC, Basrai MA. A role for histone H4K16 hypoacetylation in
724 *Saccharomyces cerevisiae* kinetochore function. Genetics. 2011;189(1):11-21. PMID: 21652526.
725 27. Holmes SG, Rose AB, Steuerle K, Saez E, Sayegh S, Lee YM, et al. Hyperactivation of
726 the silencing proteins, Sir2p and Sir3p, causes chromosome loss. Genetics. 1997;145(3):605-14.
727 PMID: 9055071.
728 28. Sunshine AB, Ong GT, Nickerson DP, Carr D, Murakami CJ, Wasko BM, et al.
729 Aneuploidy shortens replicative lifespan in *Saccharomyces cerevisiae*. Aging Cell.
730 2016;15(2):317-24. PMID: 26762766.
731 29. Glynn EF, Megee PC, Yu HG, Mistrot C, Unal E, Koshland DE, et al. Genome-wide
732 mapping of the cohesin complex in the yeast *Saccharomyces cerevisiae*. PLoS Biol.
733 2004;2(9):E259. PMID: 15309048.
734 30. Li M, Valsakumar V, Poorey K, Bekiranov S, Smith JS. Genome-wide analysis of
735 functional sirtuin chromatin targets in yeast. Genome Biol. 2013;14(5):R48. PMID: 23710766.
736 31. Kobayashi T, Horiuchi T, Tongaonkar P, Vu L, Nomura M. SIR2 regulates
737 recombination between different rDNA repeats, but not recombination within individual rRNA
738 genes in yeast. Cell. 2004;117(4):441-53. PMID: 15137938.
739 32. Stephens AD, Quammen CW, Chang B, Haase J, Taylor RM, 2nd, Bloom K. The spatial
740 segregation of pericentric cohesin and condensin in the mitotic spindle. Mol Biol Cell.
741 2013;24(24):3909-19. PMID: 24152737.

742 33. Lindstrom DL, Gottschling DE. The mother enrichment program: a genetic system for
743 facile replicative life span analysis in *Saccharomyces cerevisiae*. Genetics. 2009;183(2):413-22.
744 PMID: 19652178.
745 34. Lindstrom DL, Leverich CK, Henderson KA, Gottschling DE. Replicative age induces
746 mitotic recombination in the ribosomal RNA gene cluster of *Saccharomyces cerevisiae*. PLoS
747 Genet. 2011;7(3):e1002015. PMID: 21436897.
748 35. Moazed D, Kistler A, Axelrod A, Rine J, Johnson AD. Silent information regulator
749 protein complexes in Saccharomyces cerevisiae: a SIR2/SIR4 complex and evidence for a
750 regulatory domain in SIR4 that inhibits its interaction with SIR3. Proc Natl Acad Sci USA.
751 1997;94(6):2186-91. PMID: 9122169.
752 36. Oppikofer M, Kueng S, Martino F, Soeroes S, Hancock SM, Chin JW, et al. A dual role
753 of H4K16 acetylation in the establishment of yeast silent chromatin. EMBO J.
754 2011;30(13):2610-21. PMID: 21666601.
755 37. Heidinger-Pauli JM, Mert O, Davenport C, Guacci V, Koshland D. Systematic reduction
756 of cohesin differentially affects chromosome segregation, condensation, and DNA repair. Curr
757 Biol. 2010;20(10):957-63. PMID: 20451387.
758 38. Guacci V, Koshland D. Cohesin-independent segregation of sister chromatids in budding
759 yeast. Mol Biol Cell. 2012;23(4):729-39. PMID: 22190734.
760 39. Unal E, Heidinger-Pauli JM, Kim W, Guacci V, Onn I, Gygi SP, et al. A molecular
761 determinant for the establishment of sister chromatid cohesion. Science. 2008;321(5888):566-9.
762 PMID: 18653894.

763 40. Guacci V, Koshland D, Strunnikov A. A direct link between sister chromatid cohesion
764 and chromosome condensation revealed through the analysis of *MCD1* in *S. cerevisiae*. Cell.
765 1997;91(1):47-57. PMID: 9335334.
766 41. Spencer F, Gerring SL, Connelly C, Hieter P. Mitotic chromosome transmission fidelity
767 mutants in *Saccharomyces cerevisiae*. Genetics. 1990;124(2):237-49. PMID: 2407610.
768 42. Hickman MA, Rusche LN. Substitution as a mechanism for genetic robustness: the
769 duplicated deacetylases Hst1p and Sir2p in *Saccharomyces cerevisiae*. PLoS Genet.
770 2007;3(8):e126. PMID: 17676954.
771 43. Li M, Petteys BJ, McClure JM, Valsakumar V, Bekiranov S, Frank EL, et al. Thiamine
772 biosynthesis in *Saccharomyces cerevisiae* is regulated by the NAD^+-dependent histone
773 deacetylase Hst1. Mol Cell Biol. 2010;30(13):3329-41. PMID: 20439498.
774 44. Duan Z, Andronescu M, Schutz K, McIlwain S, Kim YJ, Lee C, et al. A three-
775 dimensional model of the yeast genome. Nature. 2010;465(7296):363-7. PMID: 20436457.
776 45. Gotta M, Strahl-Bolsinger S, Renauld H, Laroche T, Kennedy BK, Grunstein M, et al.
777 Localization of Sir2p: the nucleolus as a compartment for silent information regulators. EMBO J.
778 1997;16(11):3243-55. PMID: 9214640.
779 46. Schalbetter SA, Goloborodko A, Fudenberg G, Belton JM, Miles C, Yu M, et al. SMC
780 complexes differentially compact mitotic chromosomes according to genomic context. Nat Cell
781 Biol. 2017;19(9):1071-80. PMID: 28825700.
782 47. Belli G, Gari E, Piedrafita L, Aldea M, Herrero E. An activator/repressor dual system
783 allows tight tetracycline-regulated gene expression in budding yeast. Nucleic Acids Res.
784 1998;26(4):942-7. PMID: 9461451.

785 48. Jiang JC, Jaruga E, Repnevskaya MV, Jazwinski SM. An intervention resembling caloric
786 restriction prolongs life span and retards aging in yeast. FASEB J. 2000;14(14):2135-7. PMID:
787 11024000.
788 49. Lin SJ, Kaeberlein M, Andalis AA, Sturtz LA, Defossez PA, Culotta VC, et al. Calorie
789 restriction extends *Saccharomyces cerevisiae* lifespan by increasing respiration. Nature.
790 2002;418(6895):344-8. PMID: 12124627.
791 50. Pal S, Postnikoff SD, Chavez M, Tyler JK. Impaired cohesion and homologous
792 recombination during replicative aging in budding yeast. Sci Adv. 2018;4(2):eaaq0236. PMID:
793 29441364.
794 51. Hu Z, Chen K, Xia Z, Chavez M, Pal S, Seol JH, et al. Nucleosome loss leads to global
795 transcriptional up-regulation and genomic instability during yeast aging. Genes Dev.
796 2014;28(4):396-408. PMID: 24532716.
797 52. Song S, Johnson FB. Epigenetic mechanisms impacting aging: A focus on histone levels
798 and telomeres. Genes. 2018;9(4). PMID: 29642537.
799 53. Buchwalter A, Hetzer MW. Nucleolar expansion and elevated protein translation in
800 premature aging. Nat Commun. 2017;8(1):328. PMID: 28855503.
801 54. Mehta R, Chandler-Brown D, Ramos FJ, Shamieh LS, Kaeberlein M. Regulation of
802 mRNA translation as a conserved mechanism of longevity control. Adv Exp Med Biol.
803 2010;694:14-29. PMID: 20886753.
804 55. Janssens GE, Veenhoff LM. The natural variation in lifespans of single yeast cells is
805 related to variation in cell size, ribosomal protein, and division time. PLoS One.
806 2016;11(12):e0167394. PMID: 27907085.

807 56. Janssens GE, Meinema AC, Gonzalez J, Wolters JC, Schmidt A, Guryev V, et al. Protein
808 biogenesis machinery is a driver of replicative aging in yeast. eLife. 2015;4:e08527. PMID:
809 26422514.
810 57. Hsu HC, Wang CL, Wang M, Yang N, Chen Z, Sternglanz R, et al. Structural basis for
811 allosteric stimulation of Sir2 activity by Sir4 binding. Genes Dev. 2013;27(1):64-73. PMID:
812 23307867.
813 58. Dasgupta A, Ramsey KL, Smith JS, Auble DT. Sir Antagonist 1 (San1) is a ubiquitin
814 ligase. J Biol Chem. 2004;279(26):26830-8. PMID: 15078868.
815 59. Gardner RG, Nelson ZW, Gottschling DE. Degradation-mediated protein quality control
816 in the nucleus. Cell. 2005;120(6):803-15. PMID: 15797381.
817 60. Kriegenburg F, Jakopec V, Poulsen EG, Nielsen SV, Roguev A, Krogan N, et al. A
818 chaperone-assisted degradation pathway targets kinetochore proteins to ensure genome stability.
819 PLoS Genet. 2014;10(1):e1004140. PMID: 24497846.
820 61. Sasaki T, Maier B, Bartke A, Scrable H. Progressive loss of SIRT1 with cell cycle
821 withdrawal. Aging Cell. 2006;5(5):413-22. PMID: 16939484.
822 62. Hoggard TA, Chang F, Perry KR, Subramanian S, Kenworthy J, Chueng J, et al. Yeast
823 heterochromatin regulators Sir2 and Sir3 act directly at euchromatic DNA replication origins.
824 PLoS Genet. 2018;14(5):e1007418. PMID: 29795547.
825 63. Utani K, Aladjem MI. Extra View: Sirt1 acts as A gatekeeper of replication initiation to
826 preserve genomic stability. Nucleus. 2018;9(1):261-7. PMID: 29578371.
827 64. Yoshida K, Bacal J, Desmarais D, Padioleau I, Tsaponina O, Chabes A, et al. The histone
828 deacetylases sir2 and rpd3 act on ribosomal DNA to control the replication program in budding
829 yeast. Mol Cell. 2014;54(4):691-7. PMID: 24856221.

830 65. Kwan EX, Foss EJ, Tsuchiyama S, Alvino GM, Kruglyak L, Kaeberlein M, et al. A
831 natural polymorphism in rDNA replication origins links origin activation with calorie restriction
832 and lifespan. PLoS Genet. 2013;9(3):e1003329. PMID: 23505383.
833 66. Jessberger R. Age-related aneuploidy through cohesion exhaustion. EMBO Rep.
834 2012;13(6):539-46. PMID: 22565322.
835 67. Lister LM, Kouznetsova A, Hyslop LA, Kalleas D, Pace SL, Barel JC, et al. Age-related
836 meiotic segregation errors in mammalian oocytes are preceded by depletion of cohesin and Sgo2.
837 Curr Biol. 2010;20(17):1511-21. PMID: 20817533.
838 68. Perkins AT, Das TM, Panzera LC, Bickel SE. Oxidative stress in oocytes during
839 midprophase induces premature loss of cohesion and chromosome segregation errors. Proc Natl
840 Acad Sci USA. 2016;113(44):E6823-e30. PMID: 27791141.
841 69. Baker DJ, Jeganathan KB, Cameron JD, Thompson M, Juneja S, Kopecka A, et al.
842 BubR1 insufficiency causes early onset of aging-associated phenotypes and infertility in mice.
843 Nat Genet. 2004;36(7):744-9. PMID: 15208629.
844 70. Baker DJ, Dawlaty MM, Wijshake T, Jeganathan KB, Malureanu L, van Ree JH, et al.
845 Increased expression of BubR1 protects against aneuploidy and cancer and extends healthy
846 lifespan. Nat Cell Biol. 2013;15(1):96-102. PMID: 23242215.
847 71. North BJ, Rosenberg MA, Jeganathan KB, Hafner AV, Michan S, Dai J, et al. SIRT2
848 induces the checkpoint kinase BubR1 to increase lifespan. EMBO J. 2014;33(13):1438-53.
849 PMID: 24825348.
850 72. Uhlmann F. SMC complexes: from DNA to chromosomes. Nat Rev Mol Cell Biol.
851 2016;17(7):399-412. PMID: 27075410.

852 73. Huang J, Brito IL, Villen J, Gygi SP, Amon A, Moazed D. Inhibition of homologous
853 recombination by a cohesin-associated clamp complex recruited to the rDNA recombination
854 enhancer. Genes Dev. 2006;20(20):2887-901. PMID: 17043313.
855 74. Bitto A, Wang AM, Bennett CF, Kaeberlein M. Biochemical genetic pathways that
856 modulate aging in multiple species. Cold Spring Harb Perspect Med. 2015;5(11). PMID:
857 26525455.
858 75. Ohkuni K, Kitagawa K. Endogenous transcription at the centromere facilitates
859 centromere activity in budding yeast. Curr Biol. 2011;21(20):1695-703. PMID: 22000103.
860 76. Smith JS, Caputo E, Boeke JD. A genetic screen for ribosomal DNA silencing defects
861 identifies multiple DNA replication and chromatin-modulating factors. Mol Cell Biol.
862 1999;19(4):3184-97. PMID: 10082585.
863 77. O'Sullivan JM, Sontam DM, Grierson R, Jones B. Repeated elements coordinate the
864 spatial organization of the yeast genome. Yeast. 2009;26(2):125-38. MID: 19235779.
865 78. Nagaoka SI, Hassold TJ, Hunt PA. Human aneuploidy: mechanisms and new insights
866 into an age-old problem. Nat Rev Genet. 2012;13(7):493-504. PMID: 22705668.
867 79. Lushnikova T, Bouska A, Odvody J, Dupont WD, Eischen CM. Aging mice have
868 increased chromosome instability that is exacerbated by elevated Mdm2 expression. Oncogene.
869 2011;30(46):4622-31. PMID: 21602883.
870 80. Riesen M, Morgan A. Calorie restriction reduces rDNA recombination independently of
871 rDNA silencing. Aging Cell. 2009;8(6):624-32. PMID: 19732046.
872 81. Smith DL, Jr., Li C, Matecic M, Maqani N, Bryk M, Smith JS. Calorie restriction effects
873 on silencing and recombination at the yeast rDNA. Aging Cell. 2009;8(6):633-42. PMID:
874 19732044.

875 82. Matecic M, Smith DL, Pan X, Maqani N, Bekiranov S, Boeke JD, et al. A microarray-
876 based genetic screen for yeast chronological aging factors. PLoS Genet. 2010;6(4):e1000921.
877 PMID: 20421943.
878 83. Buck SW, Sandmeier JJ, Smith JS. RNA polymerase I propagates unidirectional
879 spreading of rDNA silent chromatin. Cell. 2002;111(7):1003-14. PMID: 12507427.
880 84. Steffen KK, Kennedy BK, Kaeberlein M. Measuring replicative life span in the budding
881 yeast. J Vis Exp. 2009;(28). PMID: 19556967.
882 85. Ausubel FM, Brent R, Kingston RE, Moore DD, Seidman JG, Smith JA, et al., editors.
883 Current Protocols in Molecular Biology. New York: John Wiley & Sons, Inc.; 2000.
884 86. Belton JM, Dekker J. Measuring Chromatin Structure in Budding Yeast. Cold Spring
885 Harb Protoc. 2015;2015(7):614-8. PMID: 26134912.
886 87. Burton JN, Liachko I, Dunham MJ, Shendure J. Species-level deconvolution of
887 metagenome assemblies with Hi-C-based contact probability maps. G3. 2014;4(7):1339-46.
888 PMID: 24855317.
889

890 ## Figure captions

891 **Fig 1. Cohesin distribution at the rDNA and centromeres in WT and *sir2*Δ cells. (A)**
892 Composite plot of Mcd1-13xMyc ChIP-Seq binding across the rDNA array from WT and *sir2*Δ
893 log-phase cells binned at 50bp resolution. **(B)** ChIP-qPCR quantifying Mcd1 enrichment at the
894 rDNA IGS1 region from log-phase cells. **(C)** Composite plot of Mcd1-13xMyc enrichment at all
895 16 yeast point centromeres. **(D)** ChIP-qPCR quantifying Mcd1 binding at two centromeres and a
896 pericentromeric site 15kb away from *CEN4*. (* $p<0.005$, two-tailed student t-test).

897 **Fig 2. Depletion of Sir2 complexes and cohesin in replicatively aging cells.** (A) Western blot
898 of Sir2 protein levels in young and aged cells. Vma2 serves as a loading control. **(B)** Depiction
899 of limiting Sir2 shared between the SIR and RENT complexes. **(C)** Western blot of Sir4 proteins
900 in young and aged cells. **(D)** Western blot of Sir3 in young and aged cells. *(E)* Western blot of
901 13x-Myc tagged Net1 in young and aged cells. **(F)** Western blot of Mcd1-13xMyc in young and
902 aged cells. **(G)** ChIP-qPCR of Mcd1-13xMyc in young and aged cells normalized to background
903 signal at an intergenic site near *PDC1*. **(H)** ChIP-qPCR of Sir4-13xMyc in young and aged cells
904 normalized to the intergenic *PDC1* site. Bud scar counts indicate the average for each enriched
905 population used for the western blotting. Qty indicates the mean western signal of each protein in
906 aged cells relative to the signal in young cells, which is set at 1.0 (n=3 biological replicates).
907 Standard errors are provided in Supplementary Fig 1B.

908 **Fig 3. Sister chromatid cohesion is weakened in old yeast cells. (A)** Representative control
909 images of arm cohesion in an *mcd1-1* mutant at permissive (25°C) and non-permissive (37°C)
910 temperatures. **(B)** Quantification of cohesion maintenance (1-dot) or loss (2-dots) from 100 cells.
911 **(C)** Representative images of young (log-phase) or aged cells arrested with nocodazole (Nz) and
912 monitored for *CENIV* arm cohesion at the *LYS4* locus. **(D)** Images of cohesion at the *CEN4* locus
913 in nocodazole-arrested young and aged cells. **(E)** Images of centromeric (*CEN*4) cohesion in
914 young and aged cells not treated with Nz. **(F)** Quantifying cohesion loss (2-dots) young cells or
915 aged cells with at least 5 bud scars (100 cells of each population). *$p<0.05$, two-tailed Fischer's
916 exact test.

917 **Fig 4. Chromosomal instability during replicative aging is linked to the rDNA. (A)**
918 Schematic of artificial chromosome loss assay for ½ sectored colonies. **(B)** Quantification of

919 sectoring frequency in young or aged WT, *sir2*Δ, *hst1*Δ, and *sir2*Δ *hst1*Δ strains. *HMR* or *FOB1*
920 were also deleted where indicated. Approximately 10,000 colonies were analyzed for each strain,
921 in several biological replicates. *p<0.05, two-tailed student t-test. **(C)** Iteratively corrected (IC)
922 and read-normalized heatmap of ChrXII Hi-C data at 10 kb resolution revealing a driving
923 interaction between *CEN12* (bin 15) and unique sequence adjacent to the rDNA (bin 45). **(D)**
924 Observed/expected statistical heatmap of ChrXII Hi-C data at 10 kb resolution using HOMER.
925 Yellow bracket indicates a putative loop structure between bins 15 and 45. **(E)** IC/read-
926 normalized Hi-C heatmap of chromosomes XI, XII, and XIII showing centromere clustering.
927 Yellow arrows indicate examples of centromere alignment with *CEN12*.

928 **Fig 5. Galactose induces CIN and shortens yeast RLS. (A)** Representative images of
929 chromosome loss (sectoring) for WT (YPH278) cells grown continuously in 2% glucose,
930 galactose, or raffinose. **(B)** Quantification of half-sector colonies for WT (YPH278) cells grown
931 on each carbon source. *p<0.01, two-tailed student t-test. **(C)** RLS assay of YPH278 cells (n=64)
932 growing on rich YEP agar plates containing either 2% glucose, galactose, or raffinose. **(D)** RLS
933 of WT (BY4741) cells (n=32) growing on 2% glucose, galactose, or raffinose.

934 **Fig 6. Modulation of RLS by manipulating *MCD1* and *SIR2* expression levels. (A)** RLS
935 assays of WT (*MCD1*$^{+}$) and *mcd1L12STOP* strains containing an integrated empty tet^{on}
936 expression vector or the same vector overexpressing *MCD1* (n=96 cells each strain). **(B)** RLS
937 assay of WT and *mcd1L12STOP* strains containing an integrated empty pRS306 vector or the
938 *SIR2* vector, pJSB186 (n=40 cells each). **(C)** RLS assay showing *MCD1* overexpression does not
939 rescue the short RLS of a *sir2Δhst1Δ* mutant. **(D)** rDNA recombination (marker loss) assay with
940 a strain bearing *ADE2* within the rDNA array. Either an empty tet^{on} vector (pRF10) or an *MCD1*

941 overexpressing version (pRF11) were integrated at the *leu2Δ1* locus of WT or *sir2*Δ versions of
942 W303AR (* p<0.05, two-tailed t-test).

943 **Fig 7. CR effects are upstream of Sir2 and Mcd1 function in old cells**. **(A)** RLS assay of WT
944 (JH5275b) and *mcd1L12STOP* (JH5276b) strains under normal 2% glucose and CR (0.5%
945 glucose) conditions (n=32 cells). **(B)** Western blot of Mcd1-13xMyc levels in young and aged
946 cells of the MEP strain RF10. Cultures were grown in YEP media containing either 2% or 0.5%
947 glucose. **(C)** Chromosome loss (sectoring) assay showing reduced sectoring in WT (YPH278),
948 *sir2*Δ (RF32), *hst1*Δ (RF33), and *sir2*Δ *hst1*Δ (RF43) strains when grown in media containing
949 0.5% glucose compared to 2%. * p<0.05, two-tailed t-test. **(D)** RLS assay of WT and *sir2Δhst1Δ*
950 mutant strains under normal and CR conditions. (n=32 cells).

951 **Fig 8. Model of residual cohesin redistribution from rDNA to centromeres in aging yeast**
952 **cells.** Centromeres of all 16 chromosomes cluster, and the rDNA remains isolated. The rDNA
953 may also contact the centromeres during anaphase, which could impact the fidelity of
954 chromosome segregation or promote recombination between the rDNA and other chromosomes.
955 Cohesin and Sir2-containing complexes are depleted in cells, but the remaining cohesin complex
956 preferentially associates with centromeres in a futile attempt to maintain sister chromatid
957 cohesion.

958

959 ## Supporting Figure and Table Captions

960 **S1 Fig. Detailed western blot and bud scar count quantification. (A)** Bar graph showing
961 average bud scar counts from young and aged cell populations used for western blotting. **(B)**

962 Detailed bud scar counts and western blot quantitation from the triplicate biological samples. **(C)**
963 Representative image of an enriched old cell population from the third Lrs4-13xMyc biological
964 replicate. Inset image allows counting of individual bud scars.

965 **S2 Fig. Western blots of additionally tested proteins from young and aged cells. (A)** A
966 13xMyc-tagged version of the Sir2 paralog, Hst1, is also depleted in aged cells. Hst1 is in a
967 complex with Sum1 and Rfm1. **(B)** The Myc-tagged Smc1 subunit of cohesin is depleted in aged
968 cells to similar levels as Mcd1. The yeast cohesin complex consists of Smc1, Smc3, Mcd1, and
969 Irr1. Smc1 and Smc3 form the coiled-coil loop structure. **(C)** A 13x-Myc tagged version of the
970 cohesin loading complex subunit, Scc2, also decreases in old cells. The cohesin loading complex
971 consists of Scc2 and Scc4.

972 **S3 Fig. RLS of the cohesion visualization strains is normal and unaffected by position of**
973 **the lacO array.** Strain 3349-1B contains a lacO array at the *LYS4* locus on Chr. IV and is used
974 as a proxy for arm cohesion, while strain 3460-2A is used to monitor centromeric cohesion 10 kb
975 away from the *CEN4* locus.

976 **S4 Fig. Confirmation of doxycycline-induced *MCD1* overexpression in WT and**
977 **mcd1L12STOP strains.** RT-qPCR of *MCD1* transcript levels relative to actin transcript levels
978 were quantified from the empty vector strains (RF146 and RF147) or the *MCD1* overexperssion
979 strains RF179 and RF180. Total RNA was isolated following 6 hours doxycycline induction
980 during log-phase growth.

981

982 **S1 Table. Yeast Strains.** This table lists each *Saccharomyces cerevisiae* strain used in the study,

983 along with its genotype and source.

984 **S2 Table. Oligonucleotides used in the study.**

Figure 1

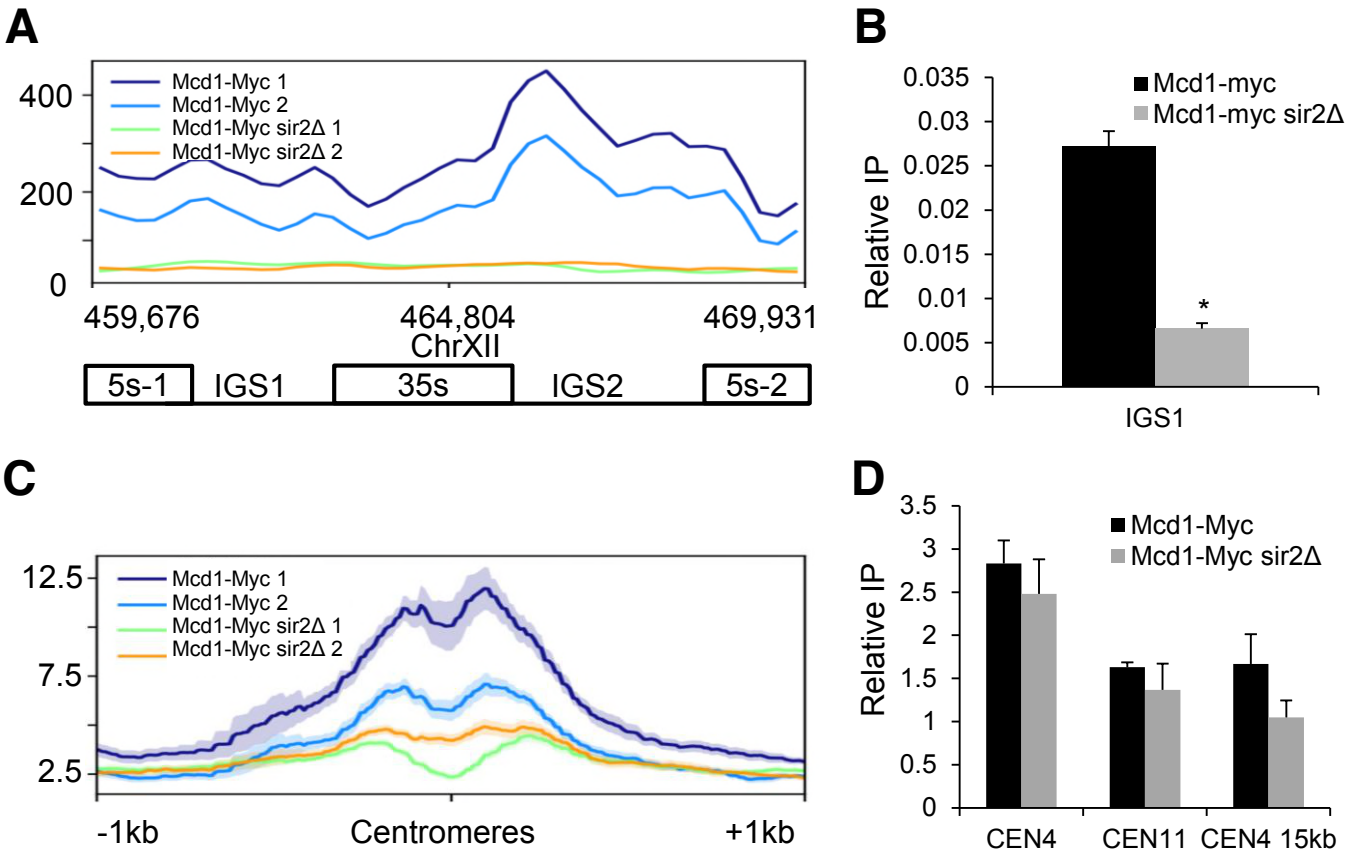
A
400
200
0
Mcd1-Myc 1
Mcd1-Myc 2
Mcd1-Myc sir2Δ 1
Mcd1-Myc sir2Δ 2
459,676
464,804
469,931
ChrXII
5s-1
IGS1
35s
IGS2
5s-2
B
0.035
0.03
0.025
0.02
0.015
0.01
0.005
0
Relative IP
Mcd1-myc
Mcd1-myc sir2Δ
*
IGS1
C
12.5
7.5
2.5
Mcd1-Myc 1
Mcd1-Myc 2
Mcd1-Myc sir2Δ 1
Mcd1-Myc sir2Δ 2
-1kb
Centromeres
+1kb
D
3.5
3
2.5
2
1.5
1
0.5
0
Relative IP
Mcd1-Myc
Mcd1-Myc sir2Δ
CEN4
CEN11
CEN4 15kb

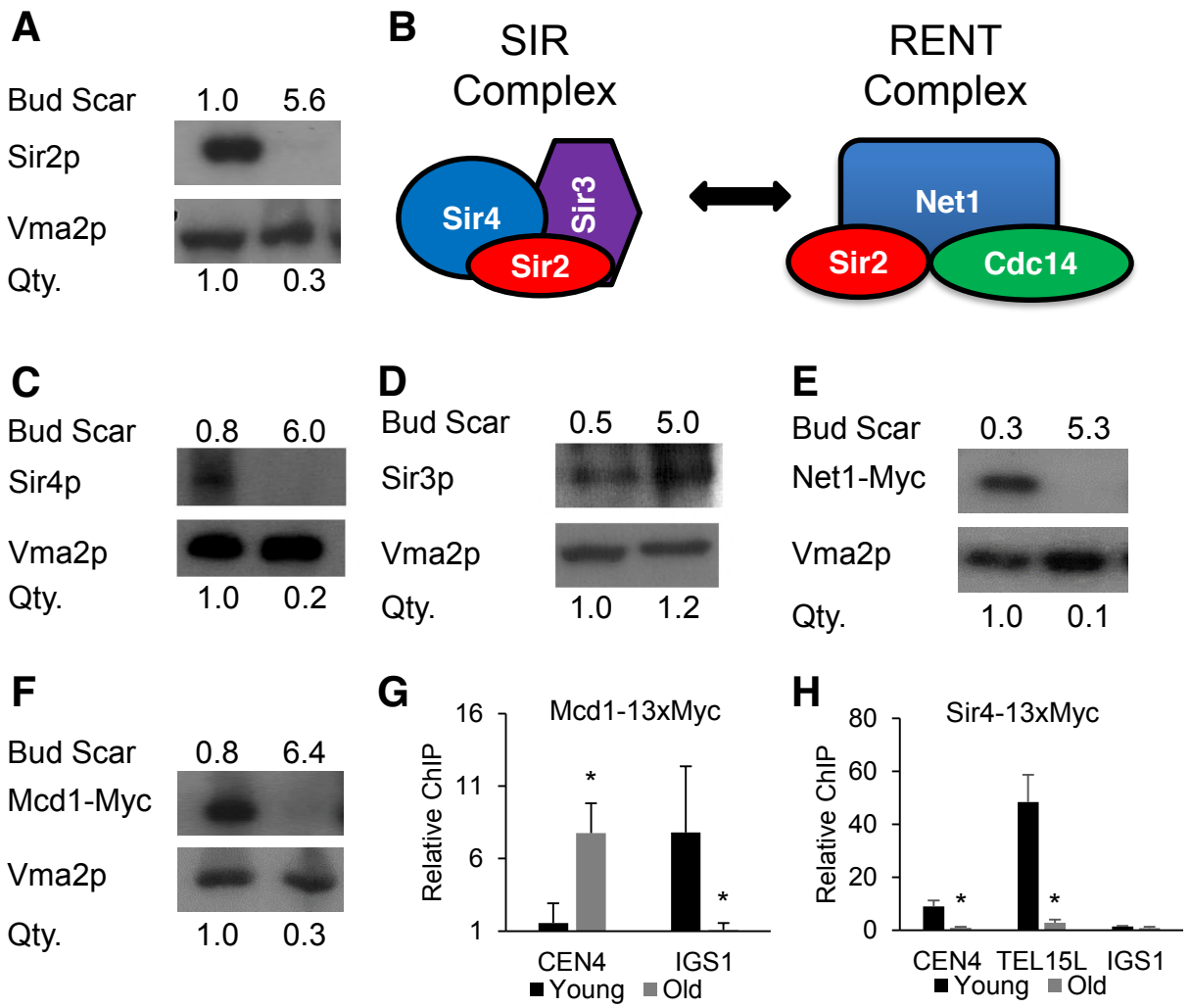
A
Bud Scar 1.0 5.6
Sir2p
Vma2p
Qty. 1.0 0.3
B
SIR Complex
Sir4
Sir3
Sir2
RENT Complex
Net1
Sir2
Cdc14
C
Bud Scar 0.8 6.0
Sir4p
Vma2p
Qty. 1.0 0.2
D
Bud Scar 0.5 5.0
Sir3p
Vma2p
Qty. 1.0 1.2
E
Bud Scar 0.3 5.3
Net1-Myc
Vma2p
Qty. 1.0 0.1
F
Bud Scar 0.8 6.4
Mcd1-Myc
Vma2p
Qty. 1.0 0.3
G
Mcd1-13xMyc
Relative ChIP
16
11
6
1
*
*
CEN4
IGS1
Young
Old
H
Sir4-13xMyc
Relative ChIP
80
60
40
20
0
*
*
CEN4
TEL15L
IGS1
Young
Old

Figure 3

A

ChrIV
Arm Cohesion (Nz)

mcd1-1 25C

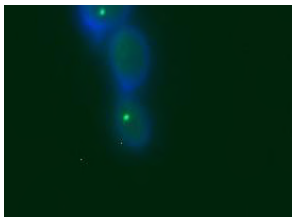

mcd1-1 37C

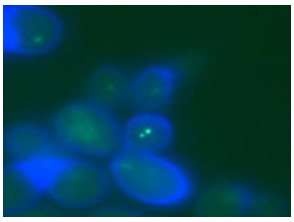

B

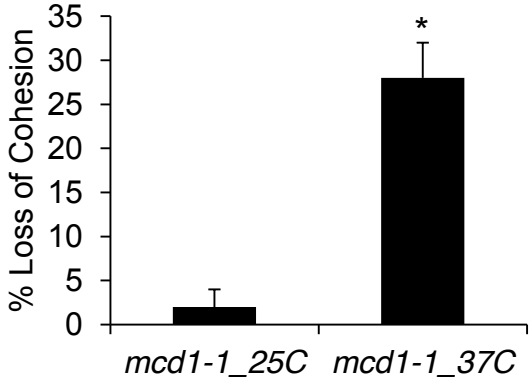

C

ChrIV
Arm Cohesion (Nz)

Young

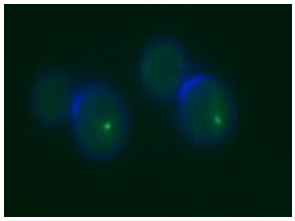

24hrs Aged

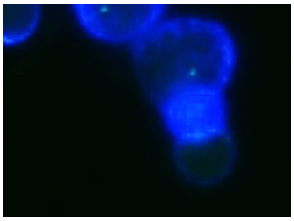

D

ChrIV
Cen. Cohesion (Nz)

Young

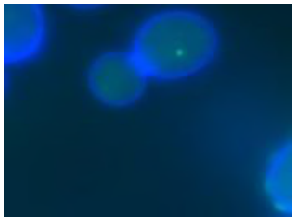

24hrs Aged

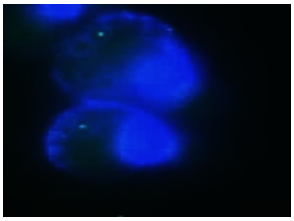

E

ChrIV
Cen. Cohesion

Young

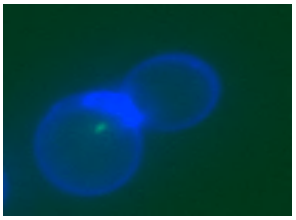

24hrs Aged

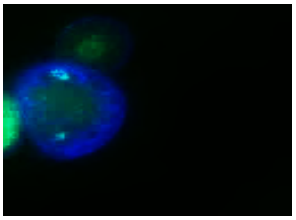

F

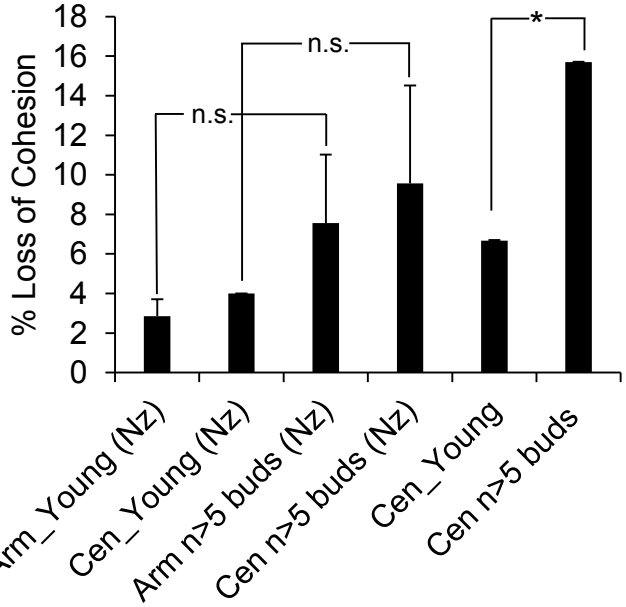

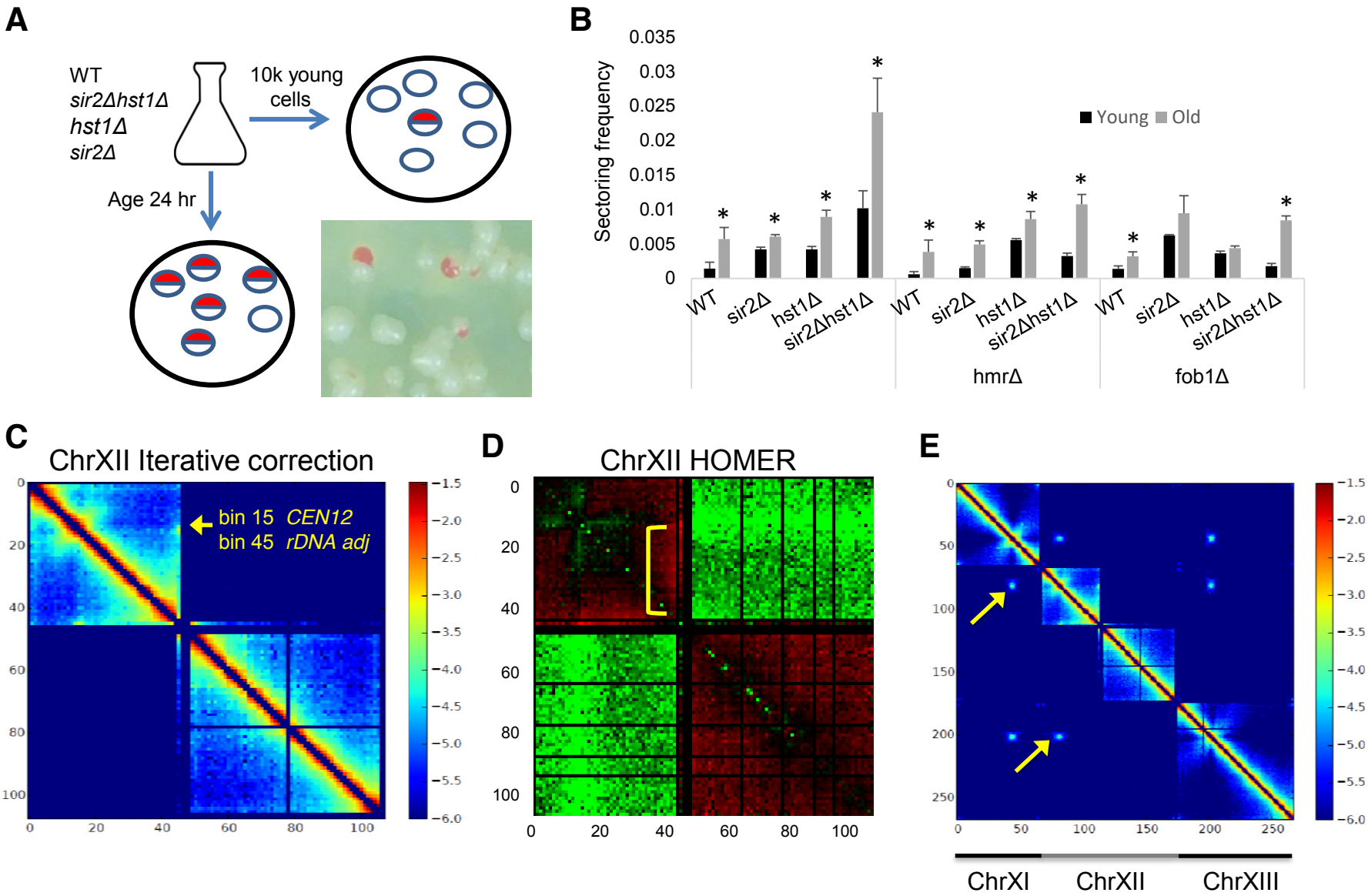
A
WT
sir2Δhst1Δ
hst1Δ
sir2Δ
10k young cells
Age 24 hr
B
Sectoring frequency
0.035
0.03
0.025
0.02
0.015
0.01
0.005
0
Young
Old
WT
sir2Δ
hst1Δ
sir2Δhst1Δ
hmrΔ
fob1Δ
C
ChrXII Iterative correction
bin 15 CEN12
bin 45 rDNA adj
D
ChrXII HOMER
E
ChrXI
ChrXII
ChrXIII

Figure 5

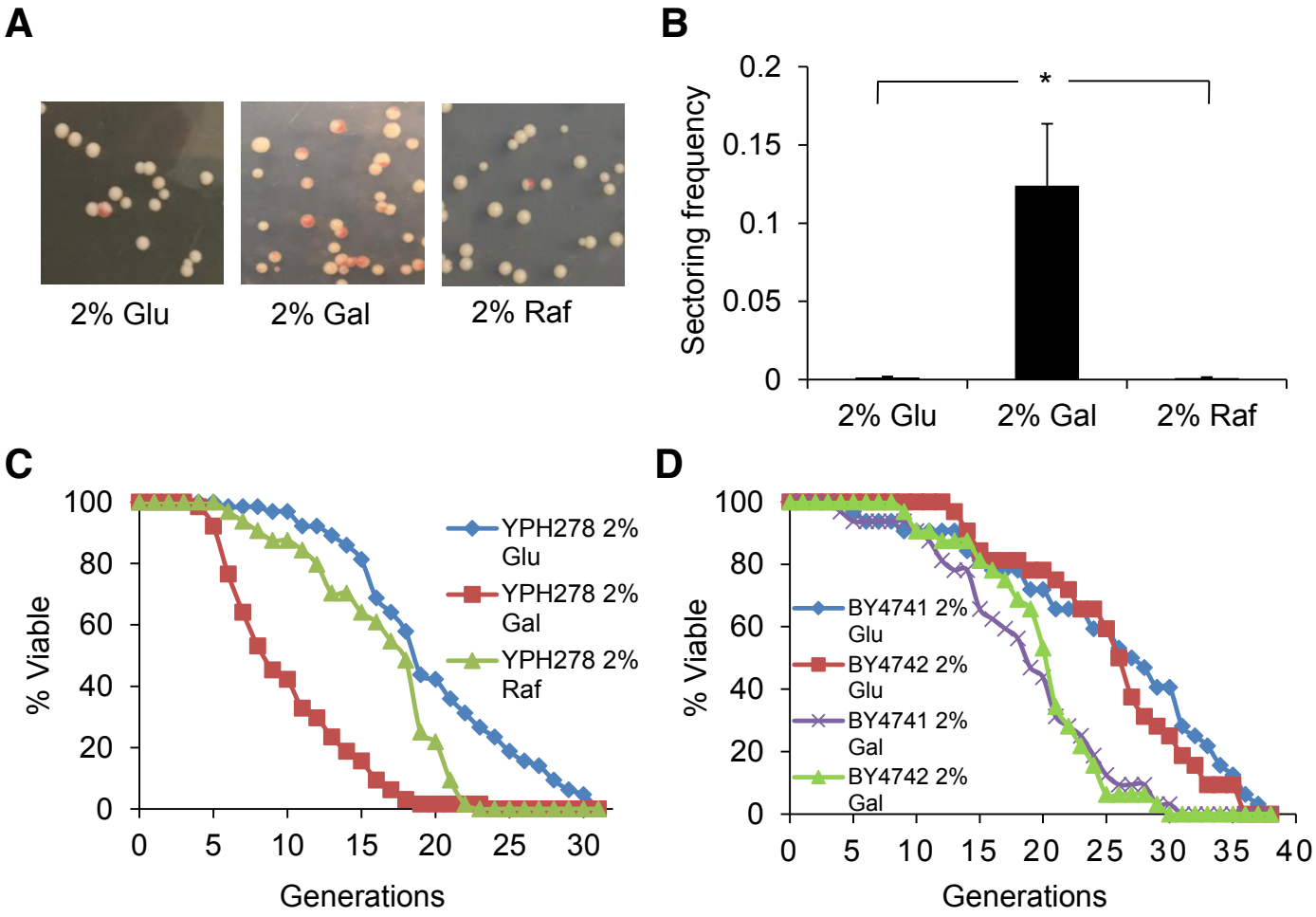
A
2% Glu
2% Gal
2% Raf
B
Sectoring frequency
0.2
0.15
0.1
0.05
0
*
2% Glu
2% Gal
2% Raf
C
% Viable
100
80
60
40
20
0
0
5
10
15
20
25
30
Generations
YPH278 2% Glu
YPH278 2% Gal
YPH278 2% Raf
D
% Viable
100
80
60
40
20
0
0
5
10
15
20
25
30
35
40
Generations
BY4741 2% Glu
BY4742 2% Glu
BY4741 2% Gal
BY4742 2% Gal

Figure 6

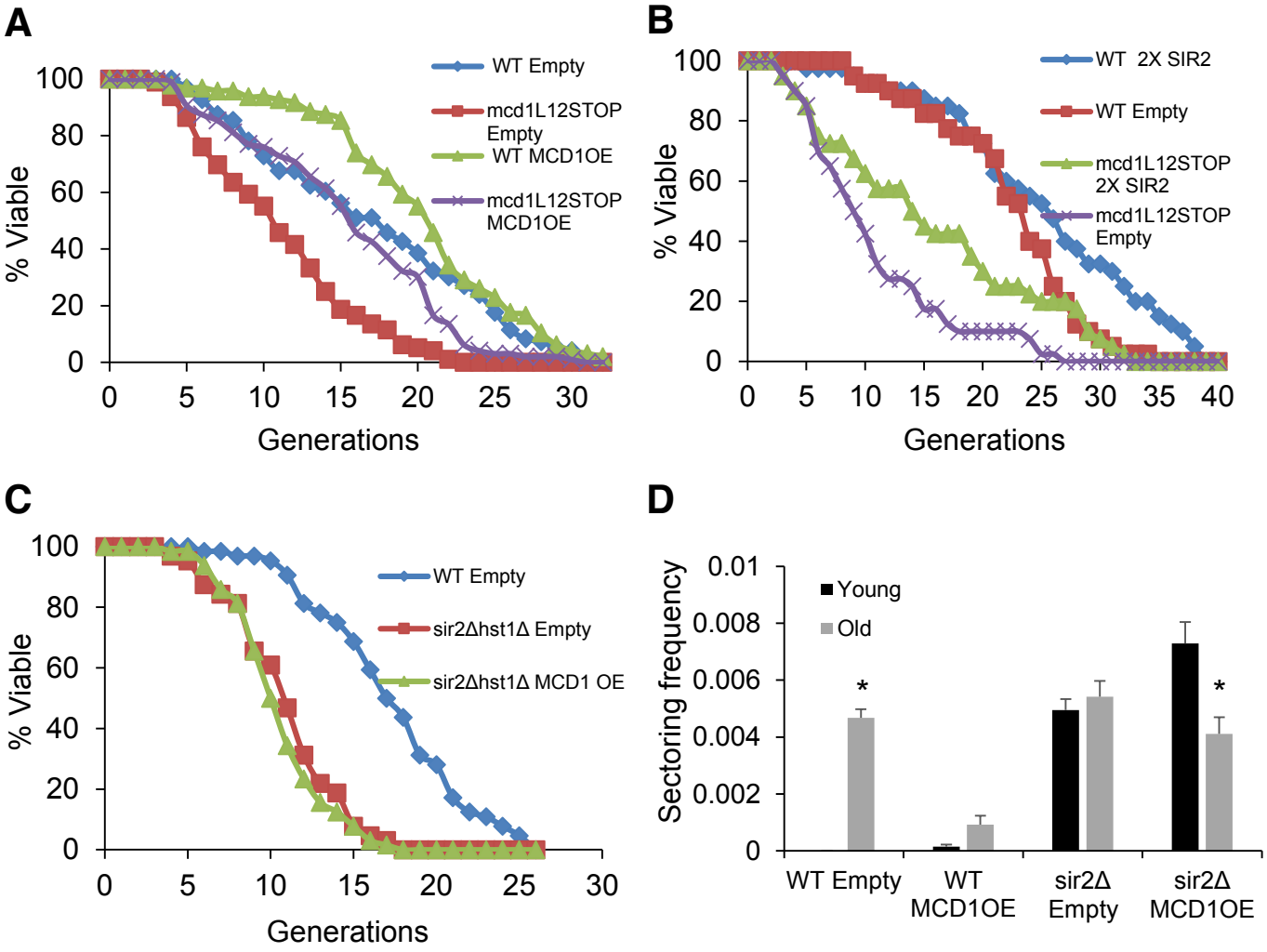
A
% Viable
Generations
WT Empty
mcd1L12STOP Empty
WT MCD1OE
mcd1L12STOP MCD1OE
B
% Viable
Generations
WT 2X SIR2
WT Empty
mcd1L12STOP 2X SIR2
mcd1L12STOP Empty
C
% Viable
Generations
WT Empty
sir2Δhst1Δ Empty
sir2Δhst1Δ MCD1 OE
D
Sectoring frequency
Young
Old
WT Empty
WT MCD1OE
sir2Δ Empty
sir2Δ MCD1OE

Figure 7

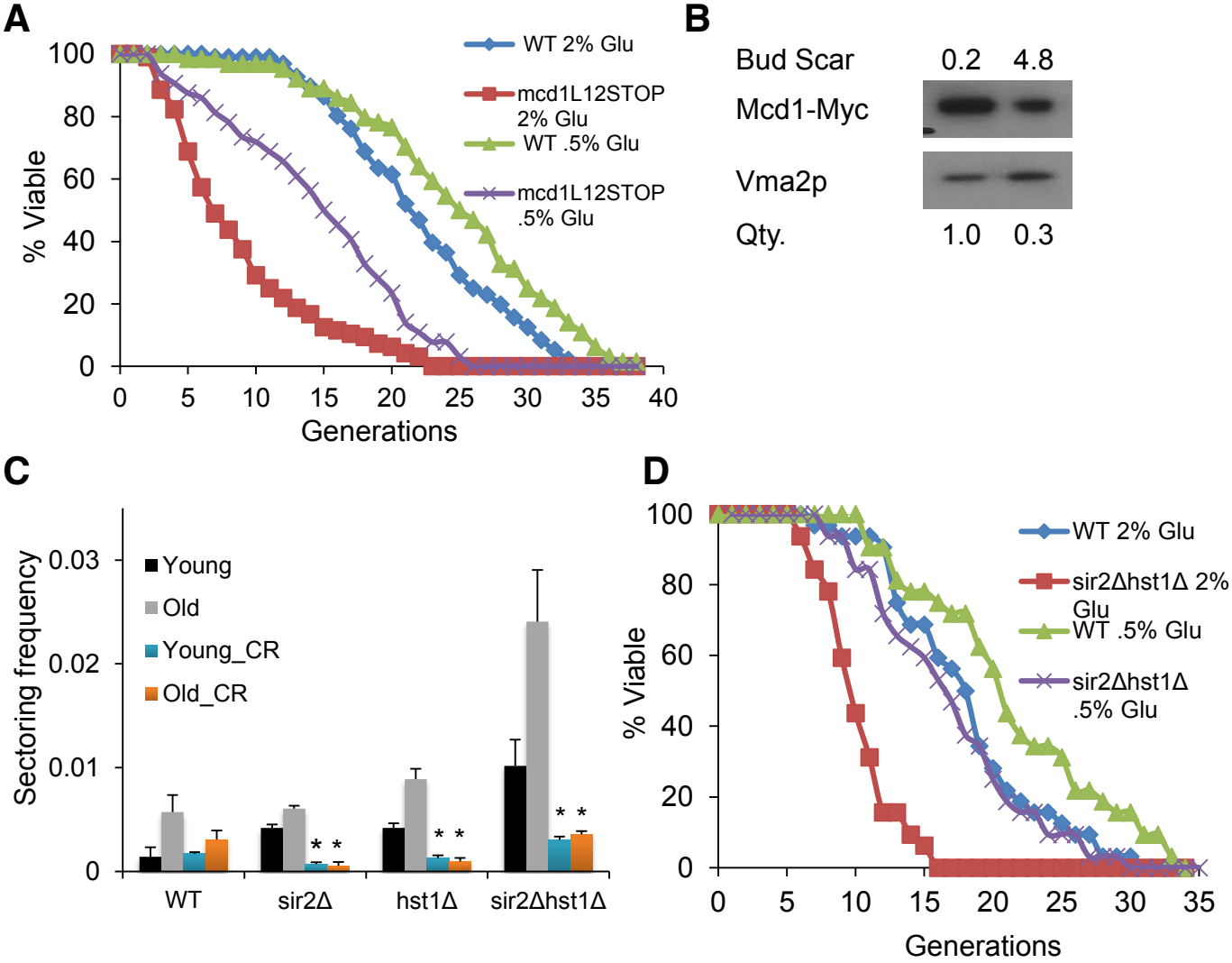
A
% Viable
Generations
WT 2% Glu
mcd1L12STOP 2% Glu
WT .5% Glu
mcd1L12STOP .5% Glu
B
Bud Scar
0.2
4.8
Mcd1-Myc
Vma2p
Qty.
1.0
0.3
C
Sectoring frequency
Young
Old
Young_CR
Old_CR
WT
sir2Δ
hst1Δ
sir2Δhst1Δ
D
% Viable
Generations
WT 2% Glu
sir2Δhst1Δ 2% Glu
WT .5% Glu
sir2Δhst1Δ .5% Glu
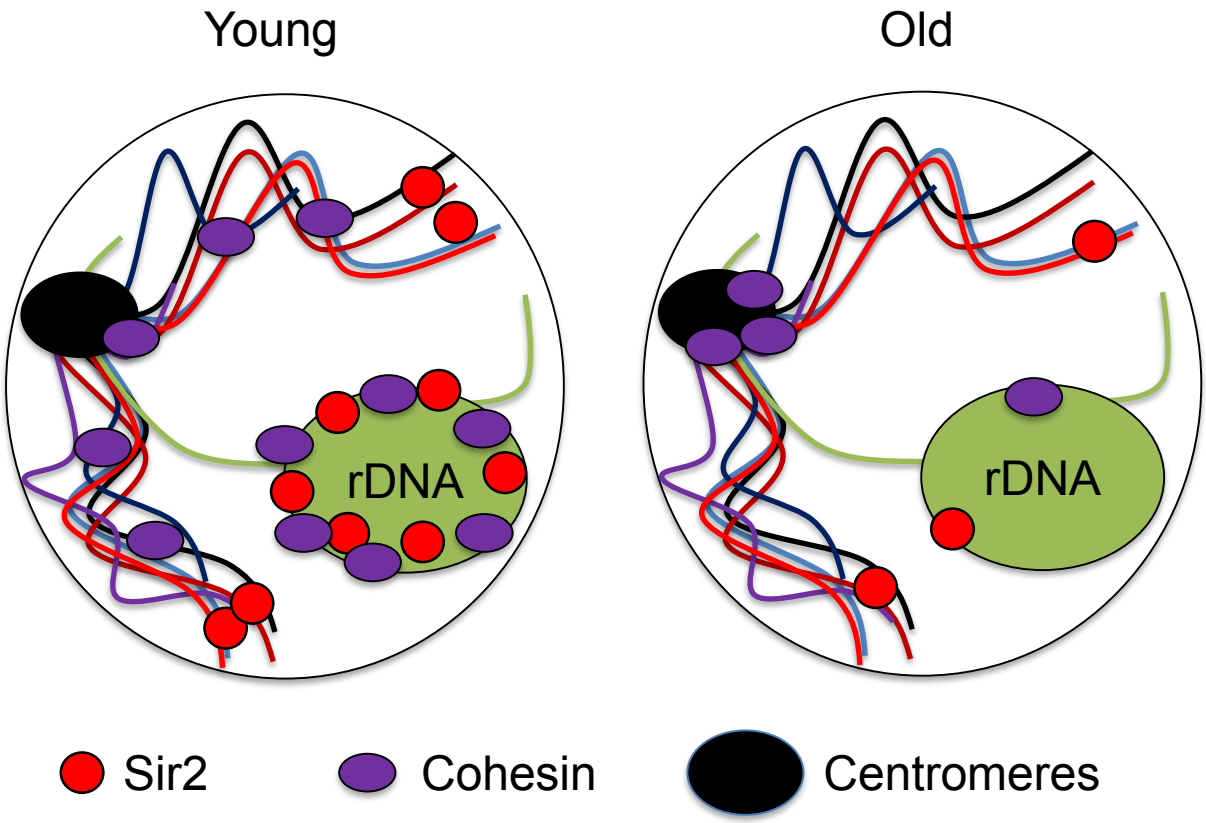
Figure 8